

Linköping University Medical Dissertations No. 977

# **A molecular approach to insulin signalling and caveolae in primary adipocytes**

**Karin Stenkula**



**Linköping University**  
**FACULTY OF HEALTH SCIENCES**

Division of Cellbiology, Department of Biomedicine and Surgery  
Faculty of Health Sciences, Linköping University  
SE-581 85 Linköping, Sweden

Linköping 2006

Cover: Fluorescence microscopic image representing a transfected primary human adipocyte expressing green fluorescent protein (GFP).

© 2006 Karin Stenkula

Published articles have been reprinted with permission from the respective copyright holder.

Printed in Sweden by LiU-Tryck, Linköping, 2006

ISSN: 0345-0082

ISBN: 91-85497-94-0

“Man blir så stark när man måste...”

Emil i Lönneberga



## ABSTRACT

The prevalence of type II diabetes is increasing at an alarming rate due to the western world lifestyle. Type II diabetes is characterized by an insulin resistance distinguished by impaired glucose uptake in adipose and muscle tissues. The molecular mechanisms behind the insulin resistance and also the knowledge considering normal insulin signalling in fat cells, especially in humans, are still unclear.

Insulin receptor substrate (IRS) is known to be important for mediating the insulin-induced signal from the insulin receptor into the cell. We developed and optimized a method for transfection of primary human adipocytes by electroporation. By recombinant expression of proteins, we found a proper IRS to be crucial for both mitogenic and metabolic signalling in human adipocytes. In human, but not rat, primary adipocytes we found IRS1 to be located at the plasma membrane in non-insulin stimulated cells. Insulin stimulation resulted in a two-fold increase of the amount of IRS1 at the plasma membrane in human cells, compared with a 12-fold increase in rat cells. By recombinant expression of IRS1 we found the species difference between human and rat IRS1 to depend on the IRS proteins and not on properties of the host cell.

The adipocytes function as an energy store, critical for maintaining the energy balance, and obesity strongly correlates with insulin resistance. The insulin sensitivity of the adipocytes with regard to the size of the cells was examined by separating small and large cells from the same subject. We found no increase of the GLUT4 translocation to the plasma membrane following insulin stimulation in the large cells, whereas there was a two-fold increase in the small cells. This finding supports the idea of a causal relationship between the enlarged fat cells and reduced insulin sensitivity found in obese subjects.

The insulin receptor is located and functional in a specific membrane structure, the caveola. The morphology of the caveola and the localization of the caveolar marker proteins caveolin-1 and -2 were examined. Caveolae were shown to be connected to the exterior by a narrow neck. Caveolin was found to be located at the neck region of caveolae, which imply importance of caveolin for maintaining and sequestering caveolae to the plasma membrane.

In conclusion, the transfection technique proved to be highly useful for molecular biological studies of insulin signal transduction and morphology in primary adipocytes.

## LIST OF PAPERS

This thesis is based on the following papers, which are referred to in the text by their Roman numerals:

- I** Stenkula Karin G., Said Lilian, Karlsson Margareta, Thorn Hans, Kjolhede Preben, Gustavsson Johanna, Söderström Mats, Strålfors Peter, Nystrom Fredrik H, *Expression of a mutant IRS inhibits metabolic and mitogenic signalling of insulin in human adipocytes. Mol. Cell. Endo. 221, 1-8 (2004)*
- II** Thorn H., Stenkula K.G., Karlsson M., Örtegren U., Nystrom F.H., Gustavsson J., Strålfors P. *Cell surface orifices of caveolae and localization of caveolin to the necks of caveolae in adipocytes. Mol. Biol. Cell 14, 3967-76 (2003)*
- III** Stenkula K G, Thorn H, Franck N, Hallin E, Sauma L, Strålfors P, Nystrom FH, *Human, but not rat, IRS1 targets to the plasma membrane in both human and rat primary adipocytes, submitted*
- IV** Franck N, Stenkula KG, Lindström T, Strålfors P, Nystrom FH, *Insulin-induced GLUT4 translocation to the plasma membrane is blunted in large compared with small primary fat cells isolated from the same subject, submitted*

## ABBREVIATIONS

EM	electron microscopy
ER	endoplasmatic reticulum
GFP	green fluorescent protein
GLUT	glucose transporter
Grb2	growth factor receptor-binding protein 2
IRS	insulin receptor substrate
MAP kinase	mitogen activated protein kinase
PH	pleckstrin homology
PI3-kinase	phosphatidyl-inositol 3-kinase
PIP	phosphatidyl-inositol-3-phosphate
PIP <sub>2</sub>	phosphatidyl-inositol-3,4-bisphosphate
PIP <sub>3</sub>	phosphatidyl-inositol-3,4,5-trisphosphate
PKB	protein kinase B
PPAR- $\gamma$	peroxisome proliferator activated receptor- $\gamma$
PTB	phosphotyrosine binding domain
SEM	scanning electron microscope
SH2	Src homology 2
SOS	son-of-sevenless
TEM	transmission electron microscope
VSFC	very small fat cells

# TABLE OF CONTENTS

<b>INTRODUCTION</b>	<b>1</b>
Insulin action and resistance	2
Adipose tissue	2
Visceral and subcutaneous fat tissues	2
Peroxisome proliferator activated receptor- $\gamma$	3
Regulation of whole body insulin-sensitivity	3
Importance of the size of adipocytes	4
<b>Insulin signalling pathways and signal mediators</b>	<b>6</b>
Insulin receptor	6
Insulin receptor substrate	7
PI3-kinase	10
Cbl/CAP complex	10
Growth factor receptor-binding protein 2	10
Glucose transporter	11
<b>Signalling through caveolae</b>	<b>12</b>
Caveolae	12
Importance of caveolae for insulin signalling	12
Caveolin	13
Distribution and importance of caveolin in caveolae	15
<b>Recombinant expression</b>	<b>16</b>
Molecular biology in the study of signal transduction	17
Fluorescent tags	17
Transfection techniques	18
Electroporation	18
Recombinant expression in adipocytes	19
<b>SPECIFIC AIMS OF THE THESIS</b>	<b>20</b>

<b>MATERIAL AND METHODS</b>	<b>21</b>
Materials	21
IRS constructs	21
Isolation of adipocytes	22
Cell culture and transfection of AG-01518	22
Separation of small and large cells	23
Electroporation	23
Measurement of Elk-1 phosphorylation	24
Sample preparations for SDS-PAGE and immunoblotting	24
SDS-PAGE and immunoblotting	25
Fluorescence microscopy	26
Immunofluorescence confocal microscopy of plasma membrane sheets	26
Electron microscopy of plasma membrane sheets	26
Electron microscopy of intact cells	27
Immunofluorescence deconvolution microscopy	28
<b>RESULTS AND DISCUSSION</b>	<b>29</b>
<b>PAPER I</b>	<b>29</b>
<b>Results</b>	<b>29</b>
Optimization	29
Insulin sensitivity	31
Importance of intact IRS function for insulin-induced signalling	31
<b>Discussion</b>	<b>34</b>
<b>PAPER II</b>	<b>35</b>
<b>Results</b>	<b>35</b>
Openings of caveolae	35
Localization of caveolin in caveolae	35
Recombinantly expressed caveolin-1 and -2	35
Caveolin distribution in human fibroblasts	37

<b>Discussion</b>	<b>38</b>
<b>PAPER III</b>	<b>39</b>
<b>Results</b>	<b>39</b>
Insulin-regulated IRS1 distribution	39
Human IRS1 in rat cells and rat IRS1 in human cells	39
PI3-kinase sensitive translocation	41
IRS1 chimera	41
<b>Discussion</b>	<b>42</b>
<b>PAPER IV</b>	<b>45</b>
<b>Results</b>	<b>45</b>
Method for separation	45
Insulin sensitivity in small and large cells	45
Amount of insulin receptor, IRS1 and caveolin-1	45
Insulin-induced activation of Akt	46
<b>Discussion</b>	<b>46</b>
<b>CONCLUSIONS</b>	<b>48</b>
<b>ACKNOWLEDGEMENTS</b>	<b>49</b>
<b>REFERENCES</b>	<b>52</b>

# INTRODUCTION

The prevalence of diabetes exceeded 150 million in the year 2000 and by the year of 2010, over 220 million people are predicted to have diabetes. The cost following this epidemic will be huge [1]. Type II diabetes accounts for the majority of patients with diabetes (90-95%), and is closely linked with obesity. The prevalence of obesity is progressing at an alarming rate due to western high-energy diet and sedentary lifestyle spreading in the West as well as in the developing world. During the last decades much effort has been spent in order to try to understand what is the exact cause of type II diabetes and also to find more effective treatments.

There are two major forms of diabetes; type I diabetes, or insulin-dependent diabetes mellitus (IDDM), and type II diabetes, or non-insulin-dependent diabetes mellitus (NIDDM) [2]. The hallmark of type I diabetes is the destruction of insulin producing pancreatic  $\beta$ -cells in an autoimmune process [2]. Type II diabetes is characterized by a resistance to insulin in the target tissues of insulin (adipose tissue, liver and skeletal muscle) in combination with failure of the pancreatic  $\beta$ -cells to produce enough of the hormone [3]. However, the exact molecular mechanisms behind the insulin resistance are unclear [4], to some extent depending on the fact that our knowledge of normal insulin signalling remains incomplete, especially in human cells.

In this thesis the insulin signalling is examined at a molecular level to gain increased knowledge of the mechanisms involved in the signal transduction in order to understand the development of insulin resistance and type II diabetes. The adipocytes function as an energy store, critical for maintaining energy balance, and constitute important targets for insulin and hence also targets for studies of the insulin signalling. A method to transfect primary human adipocytes for a molecular biologic approach is presented for the study of the localization of insulin receptor substrate (IRS) and the importance of IRS for metabolic and mitogenic control in adipocytes. Obesity strongly correlates with insulin resistance and the insulin sensitivity of the adipocytes with regard to the size of the cells is also evaluated. The insulin receptor is located and functional in the specific membrane structure, caveola. Herein, the morphology of the caveolar structure in adipocytes is therefore examined.

## **Insulin action and resistance**

Normally, following food intake, a raised blood glucose level stimulates the secretion of insulin from the pancreatic  $\beta$ -cells, which facilitates the glucose uptake in liver and peripheral tissues (muscle and adipose), while inhibiting the hepatic glucose production [5]. The insulin resistant state is distinguished by an impaired glucose uptake into the adipose- and muscle cells. Initially, the insulin-producing  $\beta$ -cells compensate the low insulin-sensitivity response by increasing the secretion of insulin but, eventually, failure of the insulin producing  $\beta$ -cells in the pancreas often occurs and results in elevated levels of blood glucose and hence manifest type II diabetes [4].

## **Adipose tissue**

Although the main part of insulin-induced glucose uptake following a meal takes place in striated muscle (80-85 %) [6], the fat tissue is central for maintaining whole body metabolic homeostasis. The adipose tissue functions as an energy depot storing triacylglycerol through insulin-induced glucose uptake and esterification of fatty acids derived from plasma lipoproteins [7], and to a minor extent, fatty acid synthesised de novo [8] (lipogenesis). When needed, the triacylglycerol is hydrolysed and released as fatty acids and glycerol (lipolysis) [9]. The release of fatty acids is regulated by insulin and catecholamines. Besides promoting glucose uptake and triacylglycerol synthesis, insulin exerts an anti-lipolytic effect by lowering the levels of intracellular cAMP, which leads to decreased phosphorylation and activity of a hormone-sensitive lipase and hence reduced hydrolysis of triacylglycerol [10, 11]. Catecholamines, on the other hand, stimulate lipolysis by binding to  $\beta$ -adrenergic receptors on the cell surface, which leads to increased cAMP, and thereby increased phosphorylation of hormone-sensitive lipase and an increased triacylglycerol hydrolysis and release of fatty acids [12].

## **Visceral and subcutaneous fat tissues**

Obesity is characterized by an increased storage of triacylglycerol in the adipose tissue. Several studies have shown that the incidence of type II diabetes rises with increased body fat content (measured as body mass index (BMI)) [13-15]. Also insulin resistance is a risk factor for the development of type II diabetes [16-18]. Adipose tissue is found in different depots in the body, and an increase of the central (visceral, intra-abdominal) depot is to a higher extent connected with insulin resistance and type II diabetes, than the

peripheral (gluteal/subcutaneous) depots [19-22]. This could be explained by visceral fat having a higher lipolytic response to catecholamines due to a higher amount of  $\beta$ -adrenergic receptors [21] and a lower response to insulin's anti-lipolytic effect [23, 24]. Also, visceral fat releases fatty acids into the portal vein and an increased visceral fat mass thus results in exposure of the liver to a high concentration of fatty acids. High concentration of circulating fatty acids has been shown to induce insulin resistance in liver and muscle [25-27] and to reduce insulin secretion from pancreatic  $\beta$ -cells [28]. The importance of the intra-abdominal fat tissue for the insulin sensitivity was demonstrated in a study where the omentum, which corresponds to less than 1 % of the total body fat mass, was surgically removed [29]. This resulted in increased insulin sensitivity, while surgical removal of a large portion (18% of total body fat mass) of the subcutaneous fat tissue did not affect the insulin sensitivity [30].

### **Peroxisome proliferator activated receptor- $\gamma$**

Peroxisome proliferator activated receptor- $\gamma$  (PPAR- $\gamma$ ) is a transcription factor that is mainly expressed in adipocytes and is important for differentiation of preadipocytes to adipocytes [31]. Activation of PPAR- $\gamma$  improves glucose and fatty acid uptake into adipocytes and stimulates synthesis of triacylglycerol [32, 33]. Thiazolidinediones, a class of anti-diabetic drugs, has a glucose-lowering effect through binding to PPAR- $\gamma$ , which results in inhibition of triacylglycerol hydrolysis and in reduced plasma levels of fatty acids [32, 34, 35]. These drugs also produce a change in the distribution of fat, with decreased amount of visceral fat and increased subcutaneous fat tissue [35-37]. Interestingly, the activity of PPAR- $\gamma$  was found to be lower in visceral fat compared with subcutaneous fat [38]. This suggests the lipolysis in subcutaneous fat tissue to be inhibited both by insulin and PPAR- $\gamma$  activity to a larger extent than in visceral fat tissue.

### **Regulation of whole body insulin-sensitivity**

The adipose tissue also functions as an important endocrine organ that produces and secretes hormones, cytokines and other peptides often referred to as adipokines, for example leptin, adiponectin, resistin, TNF $\alpha$ , IL-6 and plasminogen activator inhibitor-1 (PAI-1). These adipokines are involved in regulating whole-body energy metabolism as well as feeding and satiety [39-45]. Adipokines are also mediating effects of fat tissue on the regulation of

the whole body sensitivity to insulin. The influence of fat tissue for the whole body regulation was shown by a fat cell-specific knock out of the insulin-sensitive glucose transporter (GLUT4) in mice, which result in insulin resistance in both muscle and liver tissues [46]. A cross-talk between tissues was also evident in a study where adipocytes and myocytes were co-cultured and the release of adipokines from fat cells influenced the insulin sensitivity in the muscle cells [47].

### **Importance of the size of adipocytes**

The human adipocyte is a large cell with a diameter varying between 50 and 200  $\mu\text{m}$ . It consists of a central lipid droplet surrounded by a cytosol that is <500 nm wide. The nucleus of the fat cell protrudes since it is pushed to the side by the lipid droplet (Figure 1).

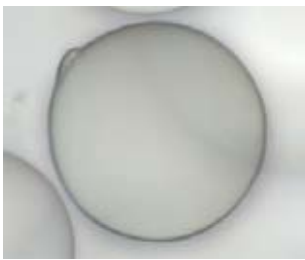


**Figure 1. Isolated human adipocyte**

Usually, obese people and individuals with type II diabetes have fat cells that are enlarged [35, 48, 49]. In severely obese individuals both the size (hypertrophy) and number (hyperplasia) of fat cells are increased [50]. The size of the adipocyte is thought to correlate with insulin sensitivity, as large fat cells are suggested to be less responsive to insulin compared with small cells [48, 51-54]. Enlarged fat cells have also been shown to secrete more TNF $\alpha$ , IL-6 and leptin, which could lead to insulin resistance [55, 56]. The size of visceral, rather than subcutaneous, fat cells has even been proposed to function as a marker for impaired insulin sensitivity [57]. However, in these previous studies comparing adipocytes of different size, large cells were obtained from obese individual and small cells from lean persons, making it hard to draw any conclusion considering the causality of the size and insulin

sensitivity of the cells. In 1972 a rather complicated method requiring several meters of dialysis tubing for size-based separation of fat cells from the same subject by flotation was used to show that the turnover rate of triacylglycerol increased with increased cell size [58]. Recently, a method for separation of fat cells into two populations, large and small, was described, which was based on both flotation and filtering techniques [59]. By micro-array analysis the expression of the immune-related genes SAA and TM4SF1 were found to be higher in the large cells [59].

## Insulin signalling pathways and signal mediators

Insulin exerts a number of effects by binding to its receptor at the cell membrane. Through metabolic signalling pathways insulin controls glucose transport, lipid, glycogen and protein metabolism and through mitogenic signalling pathways insulin can control gene transcription and cell growth (Figure 2).

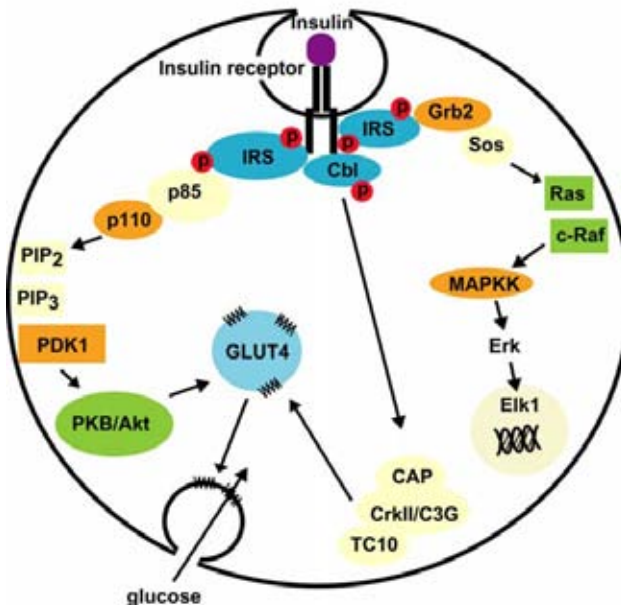


Figure 2. Schematic drawing of the major insulin signalling pathways

### Insulin receptor

The insulin receptor is a transmembrane receptor belonging to the tyrosine kinase receptor super family. The insulin receptor consists of two extracellular  $\alpha$ -subunits and two transmembrane  $\beta$ -subunits. The transmembrane  $\beta$ -units are linked to the  $\alpha$  chains by disulfide bridges and noncovalent interactions. Binding of insulin to the extra cellular  $\alpha$  domains initiates a conformational change leading to auto-phosphorylation of the

intracellular  $\beta$ -subunits, which results in increased tyrosine kinase activity against other substrates [60, 61]. Through phosphotyrosine motifs on the receptor, substrates such as insulin receptor substrate (IRS) 1-4 and Shc, can bind to the activated receptor. These substrates then become phosphorylated at several tyrosine residues and can in turn provide docking sites for Src homology 2 (SH2) domain-containing molecules such as the enzyme PI3 kinase, growth factor receptor-binding protein 2 (Grb2), and phosphotyrosine phosphatase SHP2.

### **Insulin receptor substrate**

The IRS proteins are crucial for the signal transduction in response to insulin, acting as mediators for transmission of the signal between the insulin receptor and downstream targets [62]. To some extent, in adipocytes from individuals with high risk for type II diabetes, the amount of IRS1 and degree of tyrosine phosphorylation of IRS1 is decreased [63]. A decreased IRS1 expression [64] was also found in adipocytes from subjects with type II diabetes [65]. In contrast, the amount of IRS1 was found to be similar in cells from individuals with or without type II diabetes [66]. However, in adipocytes from subjects with type II diabetes the insulin resistance was shown to occur at the level of insulin receptor phosphorylation of IRS1 leading to a reduced sensitivity for insulin stimulation of glucose uptake [64].

There are nine members identified of the insulin receptor substrate family, where the isoforms IRS1-4 are the major mediators in insulin signalling [67]. Although the IRS isoforms have similar structures (see below) and are expressed in different tissues, studies in mice with specific disruption of the IRS genes revealed that different IRS isoforms are functional in different tissues [68-73]. IRS1 is most important in adipose and muscle, while IRS2 is necessary for survival of the  $\beta$ -cells and also functions in the liver [74]. Both IRS1 and IRS2 are expressed in adipocytes and muscle, but previous findings from IRS1 deficient mice [68, 69, 75] suggest that IRS1 and IRS2 are not functionally interchangeable [76-78]. This is in line with findings in adipocytes from patients with type II diabetes, where the levels of IRS1 are decreased and IRS2 instead acts as the main mediator, albeit with impaired function [65]. IRS3 was identified in rat adipocytes as a protein associated with PI3-kinase [79]. IRS3 together with IRS1 function as substrates for the

insulin receptor in rat adipocytes [80, 81]. There is however no gene coding for IRS3 in the human genome [82].

IRS1-4 has highly conserved pleckstrin homology (PH) domains and phosphotyrosine binding (PTB) domains at the amino-termini. The PH domain binds charged head groups of specific phosphatidylinositides, thus targeting the protein to the membrane [83]. The PTB domain recognizes phosphotyrosine in the specific amino acid sequence NPXpY present in the juxtamembrane region of the insulin receptor  $\beta$ -subunit [84, 85]. The PH and PTB domains work together to target IRS to the insulin receptor [86-88]. IRS contains a number of potential tyrosine phosphorylation sites that can be activated through interaction with the active insulin receptor. Phosphorylated tyrosines in the specific amino acid sequences pYMXM and pYVNI present in IRS in turn act as docking site for the SH2 containing proteins PI3-kinase and Grb2, respectively [89] (Figure 3).

The ligand specificity of the PH domain of different IRS isoforms have been investigated by fusion-protein and binding assays, where the PH domains of IRS1, IRS2 and IRS3 were shown to have high affinity to PIP<sub>3</sub>, PIP<sub>2</sub>, and PIP, respectively [90]. In the same study the PH domains of IRS1 and IRS2 were found to translocate from the cytosol to the plasma membrane upon insulin stimulation, compared with IRS3 that was constitutively located at the plasma membrane. In another study, the tyrosine phosphorylation of IRS1 and IRS3 were examined in cells that express insulin receptor with a disrupted NPXpY motif (IR<sup>Y960F</sup>) [86]. The binding to the plasma membrane mediated by the PH domain was sufficient for insulin-stimulated tyrosine phosphorylation of IRS3, but not IRS1. The PH domains of IRS1 and IRS3 were switched, and an IRS3 chimera with IRS1 PH domain was found to have a decreased tyrosine phosphorylation in response to insulin and a similar distribution to full length IRS1 [86]. This suggests that the PH domain of IRS3 is important for the targeting of IRS3 to the plasma membrane, in a distinct way from the IRS1, which rather seemed to depend on PI3-kinase produced phosphoinositides for the subcellular targeting. Also, an intact PH domain of IRS3 was necessary for plasma membrane targeting and proper IRS3 induced glucose uptake in rat adipocytes [91]. Taylor et al [92] showed that disruption of either the PH or PTB domain of IRS1 affected the insulin-stimulated translocation of IRS1 to the plasma membrane. However, IRS1 still became tyrosine phosphorylated,

suggesting that the activation of IRS1 occurred prior to translocation to the plasma membrane [92]. In primary human adipocytes IRS1 is located at the plasma membrane already in the basal state [93]. In contrast, in rat adipocytes the IRS1 is not found at the plasma membrane in the absence of insulin stimulation [93-96].

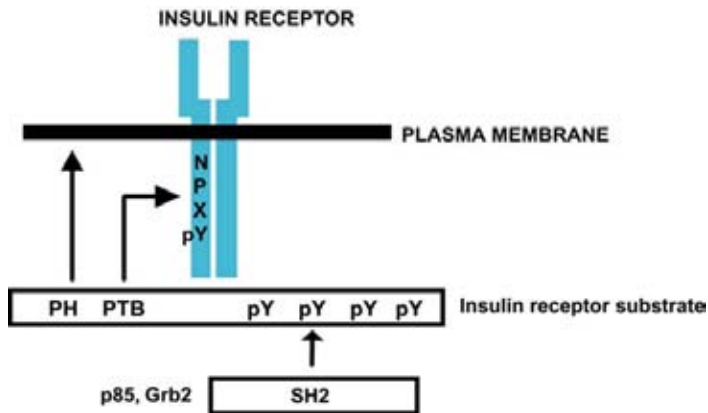


**Figure 3. Insulin receptor substrate**

A schematic illustration of the interaction of the IRS, the insulin receptor and the plasma membrane. IRS contains a PH domain, which targets IRS to the plasma membrane, and a PTB domain that recognizes a specific (NPXPY) sequence presented in the insulin receptor. IRS has a number of potential tyrosine phosphorylation sites, which can bind SH2 containing proteins such as p85 and Grb2.

In response to insulin IRS1 becomes tyrosine phosphorylated. However, IRS1 also has a large number of possible serine phosphorylation sites, proposed to have a negative regulatory function for signal transmission [97-99]. In human adipocytes, insulin-stimulated phosphorylation of IRS1 at serine 307 (corresponding to serine 302 in the mouse sequence) seems to induce a positive feedback loop, enhancing the insulin-induced signal transduction at the level of IRS1 [66]. In contrast, during long exposure to high concentration of insulin, phosphorylation of IRS at serine 312 attenuates the insulin signal, and is suggested to constitute a negative feedback regulation of the insulin signalling in human adipocytes [100].

### **PI3-kinase**

PI3-kinase is an important mediator of the metabolic signalling pathway. The PI3-kinase contains a regulatory subunit (p85) and a catalytic subunit (p110). Tyrosine phosphorylated IRS associates with the two SH2 domains of the regulatory subunit p85, which in turn binds the catalytic subunit p110. The activated PI3-kinase then goes on to phosphorylate phosphatidyl-inositols at the 3-position of the inositol-ring, generating phosphatidyl-inositol-3,4-bisphosphate (PIP<sub>2</sub>) and phosphatidyl-inositol-3,4,5-trisphosphate (PIP<sub>3</sub>) [101]. PIP<sub>3</sub> activates the phosphoinositide-dependent kinase 1 (PDK1), which will bind and activate the serine/threonine protein kinase B (PKB/Akt) [101]. Activated PKB detaches from the plasma membrane and acts through a number of different metabolic processes, including phosphorylation and activation of atypical protein kinase C  $\zeta/\lambda$  isoforms, which eventually leads to glucose uptake [102]. Also, PKB mediates phosphorylation and inactivation of glycogen synthase kinase-3, which regulates glycogen synthesis. PKB is also implicated in transcriptional control. Many of the down-stream mediators of PKB signalling are still unknown.

### **Cbl/CAP complex**

An additional PI3-kinase-independent insulin-induced signalling pathway for glucose uptake involves the proto-oncogene Cbl. The insulin receptor phosphorylates Adaptor protein containing a PH and SH2 domain (APS), which binds the SH2 domain of Cbl associated with adapter protein CAP. The signal thus mediated through the Cbl/CAP complex includes activation of CrkII/C3G and TC10, which leads to glucose transport [103-105]. This signalling pathway has been suggested to work in parallel with the PI3-kinase-dependent pathway [106].

### **Growth factor receptor-binding protein 2**

In addition to PI3-kinase also Grb2, another SH2 containing signal molecule, can bind to phosphorylated IRS. Grb2 is associated with the GDP/GTP exchange factor Son-of-sevenless (SOS). Binding of the Grb2-SOS complex, results in activation of Ras followed by phosphorylation of c-Raf, mitogen activated protein (MAP) kinase kinase (MEK1/2) and MAP kinases Erk1/2 [107]. Insulin signalling through the Ras/MAP kinase cascade, mitogenic

signalling, can control transcription factors and thus gene expression and cell growth [4, 108].

### **Glucose transporter**

Glucose transport into the cell is facilitated by glucose carrier proteins, GLUT, which are integral membrane proteins containing 12 membrane-spanning helices with both the amino and carboxy-termini at the cytoplasmic side. Binding of glucose results in a conformational change of the GLUT and a transport and release of glucose at the other side of the cell membrane.

There are 13 known members of the GLUT family, of which GLUT1-4 are the most well characterized glucose transport facilitators [109]. GLUT1 is highly expressed in erythrocytes and endothelial cells, but is present to some extent in almost all tissues. GLUT2 is present in the liver, kidney and pancreatic  $\beta$ -cells and GLUT3 is found in neurons. GLUT4 is exclusively expressed in muscle and adipose tissues and is the major insulin-responsive isoform of GLUT [110]. Insulin stimulation eventually leads to the recruitment of GLUT4 from intracellular vesicular compartments to the plasma membrane, where GLUT4 containing vesicles fuse with the membrane [111]. Notably, the GLUT1 found in muscle and fat tissue is mostly located to the plasma membrane already in the basal state, probably maintaining glucose uptake needed during basal non-stimulated conditions [112]. Under basal conditions there is equilibrium in the transport of GLUT4 from the intracellular stores to the plasma membrane and GLUT4 internalization. Insulin stimulates an increased rate of exocytosis while only slightly reducing the internalization rate [113], thereby increasing the GLUT4 content of the plasma membrane [114]. Both PI3-kinase-dependent and independent pathways control glucose transport, but all the mediators involved are still not known.

## **Signalling through caveolae**

Lipid rafts are micro-domains of the plasma membrane, which are in focus for their role in assembling signal transduction at the plasma membrane. Here, a specific subset of lipid rafts, the caveolae that is crucial for insulin signalling, is presented.

### **Caveolae**

The morphologic appearance of caveolae as small flask-shaped invaginations in the plasma membrane was described already in the 1950's [115]. Later, these invaginations were named caveolae as a description of the small caves connected with the outside of the cell [116]. They have often also been referred to as plasma lemmal vesicles [117]. Caveolae are found in most cell-types but are abundantly expressed in endothelial cells, fibroblasts, smooth muscle cells and adipocytes [118, 119]. They vary in size between 20-150 nm in diameter [120-123]. The finding of the protein caveolin as a marker for caveolae [123], made it possible to use biochemical methods for isolation and characterization of these specific membrane structures [124-126]. Caveolae are enriched in sphingomyelin, glycosphingolipids and cholesterol [127, 128], and are thereby also detergent insoluble, which provides for one means of isolating them from the rest of the membrane [129].

Caveolae have been proposed to function in several cellular events, for example in the transcytosis of endothelial cells [130]. Caveolae have also been shown to function in endocytosis, as an alternative way to clathrin-coated pit mediated endocytosis for the internalization of the simian virus 40 (SV40) [131]. Caveolae are furthermore important for maintaining the cholesterol homeostasis in the cell [132]. Recently, the uptake of oleic acid and the conversion of oleic acid to triacylglycerol were shown to take place in a specific subclass of caveolae in adipocytes [133]. In accordance with their role in organizing signal transduction a large number of signal molecules have been shown to localize to caveolae.

### **Importance of caveolae for insulin signalling**

A role of caveolae in insulin signalling was first suggested by studies in rat adipocytes where insulin was endocytosed by uncoated invaginations [134]. This was corroborated by the finding of the insulin receptor to be localized to caveolae in adipocytes [135], similarly to several other tyrosine kinase

receptors [136-138]. Insulin stimulation leads to a rapid translocation of intracellular GLUT4 to the plasma membrane, followed by a slower movement of GLUT4 to caveolae, where glucose uptake is suggested to take place [139]. Treating cells with  $\beta$ -cyclodextrin ( $\beta$ -CD) results in cholesterol depletion of the membrane and flattening of the caveolae invaginations [135, 140]. In rat adipocytes the cholesterol depletion inhibited insulin signalling in terms of decreased amount of insulin-stimulated ATP citrate lyase phosphorylation, which is implicated in the lipid synthesis, and diminished glucose uptake [135]. The mitogenic signalling of insulin was not affected, as phosphorylation of MAP kinases Erk1/2 remained intact. By adding cholesterol, the plasma membrane invaginations were again morphologically recognized and the insulin-induced signalling restored. In human adipocytes in contrast, the caveolar integrity has been shown to be necessary for both metabolic and mitogenic signalling [93]. After cholesterol depletion by  $\beta$ -CD treatment insulin-stimulated phosphorylation of the insulin receptor and IRS1 was still operational in the plasma membrane, but failed to mediate the signal further downstream to enhanced phosphorylation of PKB and Erk1/2, and glucose uptake [93].

### **Caveolin**

Caveolin was first identified as a substrate of the Rous sarcoma viral oncogene v-src [141]. Another group identified the same protein, named VIP-21, as a component of the trans-Golgi network [142]. The caveolin protein was then identified as a structural protein of caveolae [123]. There are several isoforms of caveolin (1 $\alpha$  and  $\beta$ ; 2  $\alpha$ ,  $\beta$ , and  $\gamma$ ; 2 and 3) [143-147]. The caveolin-1 $\alpha$  isoform is often referred to simply as caveolin. Caveolin-1 and -2 are expressed in most cell types to the same extent, but caveolin-3 is predominantly expressed in muscle cell types [148].

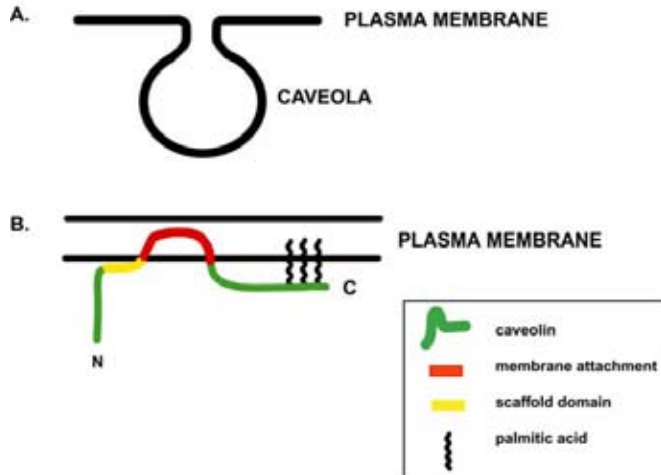


**Figure 4. Caveolae and caveolin**

A) Caveola shown as a plasma membrane invagination.

B) The caveolae marker protein caveolin forms a hairpin structure in the plasma membrane. Both the amino and carboxyl termini of caveolin are facing the cytoplasm.

Specific domains of the caveolin protein regulate the structure and function of caveolin. The 18-24 kDa caveolin forms a hairpin-structure in the membrane through a 33 amino acid membrane-attachment domain (residues 102-135), with both the amino and carboxyl termini facing the cytoplasm (Figure 4). Caveolin also contains an oligomerization domain (residue 61-101) necessary for oligomer formation as caveolin-1 forms homo-oligomers of 14-16 monomers in the endoplasmic reticulum (ER) [149]. They in turn interact to form larger complexes that are transported to the plasma membrane. Caveolin-2 is unable to form homo-oligomers and instead forms hetero-oligomers with caveolin-1 enabling its transport to the plasma membrane via Golgi [150, 151]. Within the oligomerization domain is the caveolin scaffold domain (CSD, residues 82-101), implicated in the interaction with other signal molecules [152, 153] and also found to be necessary for the membrane insertion of caveolin [154]. Interestingly, in a peptide-binding study the CSD, but not the membrane-attachment domain, was shown to be essential for the membrane attachment of caveolin-1 [155].

Two caveolin-binding motifs ( $\phi$ XXXX $\phi$ XX $\phi$  and  $\phi$ XX $\phi$ XXXX $\phi$ , where  $\phi$  is an aromatic amino acid) have been identified by phage display libraries [152]. These motifs are found in almost all caveolin-associated proteins. The finding of one such motif ( $^{1220}$ WSFGVVLW $^{1227}$ ) in the insulin receptor  $\beta$ -subunit triggered functional studies of caveolin and insulin receptor interaction [156]. After mutation within the CSD of the insulin receptor, the mutated receptor was poorly expressed and did not become autophosphorylated [157]. A knock-out model of mice lacking caveolin-1 has provided further insight into the caveolin-1 deficient state [158, 159]. Phosphorylation of insulin receptor and several down-stream signalling molecules were reduced specifically in adipocytes, but not in muscle and liver [160]. The expression of insulin receptor was reduced, although with unchanged mRNA-levels, which indicated that caveolin might be important for the stabilization of the insulin receptor.

As mentioned before, caveolae are enriched in cholesterol and caveolin-1 binds cholesterol specifically in a 1:1 ratio [161]. Caveolin-1 and -3 are palmitoylated on three cysteine residues at the carboxyl end, which is necessary for binding and transport of cholesterol from the ER to the plasma membrane [162, 163]. A further domain, the signature domain (residues 66-71) is also necessary for the transport of cholesterol from ER [164].

### **Distribution and importance of caveolin in caveolae**

In morphological studies of caveolae, the caveolae marker protein caveolin has been reported to be located in the caveolar bulb [123, 165, 166], forming a striated coat [123, 165, 167]. However, this striated formation was not found in another study [166], instead labelling against caveolin was found at distinct regions of the caveolar structure, mainly at the membrane attachment area, in a ring-like formation [166]. This discrepancy might be due to different techniques during preparation. The caveolin coat has previously been studied thoroughly by Peters et al [165] and Rothberg et al [123]. Peters et al used the technique of critical point drying and coating of the specimen with a thin layer of chromium. The critical point drying technique is known to induce shrinkage of the specimen [168], which might have caused the striated formation. Rothberg et al used platinum and carbon to build up a replica, and platinum is known to induce decoration artefacts, which might have been strengthened by the additional layer of carbon. Westermann et al [166] used a

freeze fracture-replica method, where the membrane structure is stabilized prior to gently dissolving the unfractured cell components by SDS treatment.

Caveolin has been proposed to drive the formation of caveolae by being involved in the actual bending of the membrane or, alternatively, to be necessary for the stabilization of the caveolar structure [169]. Expression of caveolin-1 in cells lacking caveolae induces the formation of caveolar structures [170, 171]. However, in caveolin-2 deficient mice the loss of caveolin-2 did not result in a loss of the formation of caveolae [172], and caveolin-2 is not thought of as necessary for the caveolae formation. The formation of caveolae has been suggested to occur in the plasma membrane [170], but recently, another hypothesis based on light microscopy studies of the translocation of newly synthesized caveolin, localizes caveolae formation to the Golgi complex [173].

## **Recombinant expression**

One of the basic techniques for molecular biological studies is recombinant expression. The DNA of interest is inserted (by restriction enzymes) into a plasmid (expression vector). The plasmid contains a promoter to drive the production of mRNA from the inserted DNA to obtain a recombinant expressed protein. The plasmid is transferred into eukaryotic cells by transfection. The DNA insert, coding for the gene of interest, is often fused to an epitope tag, for example Myc or HA, which is a short amino acid sequence that makes it possible to trace the recombinant expressed protein by detection with antibodies directed against the tag. There are also fluorescent tags (for example green fluorescent protein, GFP) that are useful for detection by microscopic techniques.

By antisense technology there are three ways to inhibit the expression of a specific gene at the RNA level; single stranded antisense oligonucleotides, activation of RNA cleavage by catalytically active oligonucleotides (named ribozymes), and small interfering RNA molecules [174]. Conversely, the amount of a particular protein can be increased by recombinant over-expression, thereby increasing the protein level. Another way to regulate a specific gene at the protein level is by recombinant expression of a dominant negative gene construct inserted into a plasmid. The expressed dominant

negative protein will interfere with the functional normal endogenous protein. The plasmid carried DNA encoding for a gene of interest can be manipulated by introduction of point mutations at specific sites to cause deletion/substitution of specific amino acids, or manufactured to create truncated forms or specific peptide sequences.

### **Molecular biology in the study of signal transduction**

During the last decades the use of molecular biological techniques in the research of insulin signalling has exploded, as in the whole field of cell biology, and has brought deeper knowledge of the molecular mechanisms of cell function and signal transduction. For example, as already mentioned, recombinant expression of caveolin-1 in caveolin-deficient cells is sufficient to induce formation of caveolae [170]. Fusion proteins of for instance the PH domain of IRS with an epitope-tag have been useful for binding-assays and for visualization of subcellular localization [90, 92]. In rat adipocytes overexpression of IRS1 2, 3, or 4 was shown to be sufficient to induce translocation of GLUT to the plasma membrane without insulin stimulation [175-177]. Furthermore, expression of an antisense ribozyme towards IRS1 markedly decreased GLUT4 translocation in response to insulin [176].

### **Fluorescent tags**

The use of fluorescent tags has opened up a new dimension for microscopic techniques where movement and subcellular localization of tagged proteins can be traced in fixed or even living cells. The dynamic processes involving caveolae in response to binding and internalization of SV 40 were visualized by tracing fluorescent-tagged caveolin-1 in living cells [173]. The caveolin-1-labelled structures were traced from the Golgi to the plasma membrane, suggesting that formation of caveolae occurs in Golgi [173]. The disruption of caveolae by expressing a caveolin-1 mutant (Cav1/S80E), known to interfere with the caveolae organization, partly inhibited the endocytosis of GLUT4 [178]. Thus, GLUT4 seems to require an intact caveolar structure for proper trafficking. A system, built on GFP fused with the substrate domains of protein kinases can visualize protein phosphorylation in response to insulin, which makes it possible to actually follow the phosphorylation cascade in different cellular compartments [179]. In response to insulin, for example, the subcellular localisation of yellow fluorescent protein tagged PKB was traced to Golgi [180].

Some caution should be taken when using manipulated DNA; especially the epitope-tag has to be properly fused to avoid misinterpreting results. In a study of the transport of SV40 through caveolae, caveolin-1 was fused with GFP either at the amino- or carboxyl termini. In cells expressing caveolin-1-GFP the SV40 uptake was shown to be functional, but was inhibited in cells expressing GFP-caveolin-1 although the distribution of both caveolin forms were similar according to fluorescence microscopical investigations [181].

### **Transfection techniques**

There are different techniques for transfection, virus and non-virus mediated. The choice of method depends on the cell type and the transfection efficiency needed. The virus-mediated method usually results in high transfection efficiency in most cell types, but has the disadvantage of being hazardous to handle. On the other hand, the non-virus methods are usually less efficient and also cause cell death to a greater extent, but still they are often preferred as they are less cumbersome [182]. There are several non-virus mediated transfection techniques, calcium phosphate co-precipitation [183], microinjection [184], lipofection [185], and electroporation [186]. Lipofection, or liposome transfection, is frequently used, and is based on lipid-mediated DNA transfer by creating DNA-containing lipid vesicles, liposomes, which easily merge with the cell membrane [185]. During cell division the cell's nuclear membrane dissolves which makes it easier for the DNA to enter the nucleus.

### **Electroporation**

Today, transfection by electroporation is very common as the method in general generates high transfection efficiency. Neumann et al first published the electroporation method in 1982 for gene transfer into murine cells in a homemade electroporation chamber [186]. The method was thereafter mainly used for transfection of bacteria, where only a single transfected bacterium was necessary for generation of transfected clones. At that stage, as not that much concern was taken considering cell viability, the method was regarded as quite rough. Since then, the electroporation method has been refined by optimization of protocols and technical improvements of equipment, to allow transfection by electroporation of eucaryotic cells [187-189].

Electroporation involves transient permeabilization of the cell membrane, by application of an external electric field that leads to a reversible break down of the membrane [190, 191]. The permeabilized membrane allows DNA transfer by electrophoretic forces [192]. The DNA is then proposed to enter the nucleus by an active ATP dependent mechanism, [193]. The transfer of exogenous DNA from the cytosol to the nucleus, rather than the transfer across the cell membrane, has been in focus lately [194]. Recently, a way for nucleofection by direct transfer of DNA into the nucleus of the cell, based on electroporation is commercially available (Amaxa, Cologne, Germany). The method is claimed to generate high transfection efficiency of most cell types, and is also easy to use, as the protocols are pre-designed for different cell types by the supplier.

### **Recombinant expression in adipocytes**

A molecular biological approach to insulin signalling studies is often performed in the immortalized 3T3-L1 cell-line, which obtains an adipose phenotype after drug-induced differentiation. Several ways for transfection of differentiated 3T3-L1 adipocytes have been published, for example by electroporation [195], or virus-mediated transfection [196]. Yet, the induced differentiation of 3T3-L1 has been reported as non-uniform [197]. The electroporation technique has been applied for studies of the role of IRS for metabolic control in primary rat adipocytes [176, 177, 198], which are more physiologically relevant compared with immortalized cell-lines as 3T3-L1. However, no transfection protocol has been published for transfection of primary human adipocytes, which would be the most physiologically relevant adipose model for clinical implications.

## **SPECIFIC AIMS OF THE THESIS**

To develop and optimize a method for transfection of primary human adipocytes.

To use the transfection technique to study the importance of IRS for insulin-induced metabolic and mitogenic signalling and the localization of IRS1 in primary human adipocytes.

To use the transfection technique to study the distribution of caveolin-1 and -2 in caveolae of primary fat cells.

To examine the importance of the size of adipocytes from the same subjects for insulin signalling, including GLUT4 translocation.

## MATERIAL AND METHODS

### Materials

Rabbit anti-IRS1, anti-caveolin-1 and -2, and anti-phospho-Akt1/PKB $\alpha$  polyclonal antibodies, mouse anti-caveolin-1 and -2 monoclonal antibodies were from Upstate Biotechnology (Charlottesville, VA, USA). Rabbit anti-IR $\beta$ , anti-GLUT4, anti-myc, anti-HA polyclonal antibodies from Santa Cruz Biotechnology (CA, USA) and rabbit anti-phospho-ERK p44/p42 polyclonal antibody from Cell Signaling Technology (Beverly, MA, USA). Mouse anti-HA monoclonal antibodies were from Covance (Berkley, CA, USA).

The pCIS2-IRS-3F4 construct, pCIS2-HA-IRS1, pCIS2-HA-Erk and empty pCIS2 vector was a kind gift from M.J. Quon, NCCAM, NIH, (Bethesda, MD, USA). Sources or construction of pCIS2-myc-caveolin-1 and -2, pCIS2-HA-PKB/Akt, pCB7-myc-caveolin-1, pCDNA3-myc-caveolin-1 pCB7 and pCIS2-eGFP have been presented earlier [199]. The rat IRS1 (pCMVhis/IRS-1) was a kind gift from Xiao Jian Sun, Harvard Medical School (Boston, MA USA). The pRluc was from BioSignal Packard (CT, USA).

### IRS constructs

The carboxy-terminus of pCMVhis/IRS-1 was amplified upstream of the EcoRI site at position 2695 and downstream of the stop codon by PCR. The product underwent an additional round of PCR using a reverse primer with a built in HA-tag, stop codon and a restriction site for XhoI. The resulting product was then cut and isolated with EcoRI and XhoI. The remaining N-terminal fragment of IRS1 was cut from the pCMVhis/IRS-1 plasmid using ClaI and EoRI. The two fragments were joined and then ligated into the ClaI and XhoI site of the pCIS2 plasmid. Restriction enzyme cleavage and DNA sequencing verified the integrity of the new pCIS2-HA-rat IRS1 construct. The HA-tagged rat IRS1/human carboxy-terminus was constructed as follows. Two EcoRV sites were created in pCIS2-HA-rat IRS1 by site-directed mutagenesis. The carboxy-terminal amino acids were cut by EcoRV digestion and the large pCIS2-HA-rat IRS1 fragment was isolated. The corresponding carboxy-terminal human sequence was amplified from pCIS2-HA-human IRS1 by PCR, and the product inserted in the EcoRV digested pCIS2-HA-rat IRS1 fragment by ligation. The HA-tagged rat IRS1/human

carboxy-terminus (pCIS2-HA-r/h44aa-IRS1) in the vector pCIS2 was verified by DNA sequencing.

### **Isolation of adipocytes**

Subcutaneous abdominal human adipose tissue was removed during surgery. The patients were women operated for various gynaecological diseases, usually requiring hysterectomy. Patients were not investigated with regard to insulin sensitivity, but subjects with the diagnosis of diabetes mellitus were excluded. The adipose tissue was cleared from vascular and fibrous structures and rinsed in 0.9 % (w/v) NaCl. The fat tissue (5-15 g) was cut with scissors into millimetre-sized pieces and digested in equal volume (1g/ml) of Krebs-Ringer solution (0.12 M NaCl, 4.7 mM KCl, 2.5 mM CaCl<sub>2</sub>, 1.2 mM MgSO<sub>4</sub>, 1.2 mM KH<sub>2</sub>PO<sub>4</sub>) containing 20 mM HEPES, pH 7.4, 3.5 % (w/v) fatty acid-free bovine serum albumin, 200 nM adenosine, 2 mM glucose and 260 U/ml collagenase (Worthington Lakewood, NJ, USA) for 1.5 h at 37 °C in a water bath with agitation. After collagenase digestion the adipocytes were separated from connective tissue debris by filtering through a gauze. The adipocytes were then washed (at 40 % cells by volume) in the Krebs-Ringer solution containing 20 mM HEPES, pH 7.4, 1% (w/v) fatty acid-free bovine serum albumin (Roche, Mannheim, Germany), 200 nM adenosine and 2 mM glucose, allowed to float by gravity during rinsing, and then kept in a water bath with agitation at 37 °C.

Rat adipocytes from the epididymal adipose tissue of Harlan Sprague Dawley rats (130–160 g, B&K Universal, Sollentuna, Sweden) were isolated by collagenase digestion (described above, except that the cells were centrifuged during rinsing). Cells were incubated in Krebs-Ringer solution (0.12 M NaCl, 4.7 mM KCl, 2.5 mM CaCl<sub>2</sub>, 1.2 mM MgSO<sub>4</sub>, 1.2 mM KH<sub>2</sub>PO<sub>4</sub>) containing 20 mM HEPES, pH 7.40, 1% (wt/vol) fatty acid-free bovine serum albumin, 100 nM phenylisopropyladenosine, 0.5 U · ml<sup>-1</sup> adenosine deaminase with 2 mM glucose, at 37°C on a shaking water bath.

### **Cell culture and transfection of AG-01518**

Human foreskin fibroblasts AG-01518 were grown on gold-grids in DMEM supplemented with 50 UI/ml penicillin, 50 µg/ml streptomycin, and 10% (vol/vol) newborn calf serum in 10% CO<sub>2</sub>. For transfection, fibroblasts were transferred to medium without antibiotics and the following day were

transfected with 1  $\mu\text{g}$  pcis2 caveolin-1 and Lipofectamine 2000 (Invitrogen) in 600  $\mu\text{l}$  for 5 h, according to the provided protocol (Invitrogen, Carlsbad, CA). The cells were then incubated for a further 24 h in medium without antibiotics.

### **Separation of small and large cells**

The separation of isolated adipocytes into small- and large fractions was achieved using nylon filters (Millipore, Billerica, MA, USA). In order to collect the small adipocyte fraction, 1ml of fat cells was suspended in 45 ml of fresh medium and gently filtered through a filter with a pore size of 60  $\mu\text{m}$ . The adipocyte suspension that was trapped on this filter was passed through a second filter with a pore size of 120  $\mu\text{m}$ . The adipocytes that were retained on this second nylon filter were collected and constituted the fraction of large adipocytes. Aliquots from each fraction were stained using Mayer's Haematoxylin allowing visualisation of their nuclei in order to distinguish adipocytes from other particles such as lipid droplets. The cell diameter of the adipocytes was measured using Scion Image (Scion Corporation, Frederick, Maryland, USA). Representative pictures were taken at 10-20x magnification using E800 Eclipse Microscope (Nikon, Japan) or a Leica, DMRXA2, (Leica, Wetzlar, Germany).

### **Electroporation**

Briefly, each 0.4-cm gap electroporation cuvette was filled with 200  $\mu\text{l}$  of the adipocyte solution and an additional 200  $\mu\text{l}$  of PBS buffer (137 mM NaCl, 2.7 mM KCl, 10 mM  $\text{Na}_2\text{HPO}_4$ , 1.8 mM  $\text{KH}_2\text{PO}_4$ , pH 7.5) containing plasmid DNA as indicated in the text. For human adipocytes, each cuvette was electroporated with six exponentially decaying pulses, at voltages described in the text, at 25  $\mu\text{F}$  or with one square-wave pulse at 400 V 4 msec using a Bio-Rad GenePulser II (Bio-Rad Laboratories Inc., Hercules, CA, USA). For rat adipocytes each cuvette was electroporated with six exponentially decaying pulses, at 600 V, 25  $\mu\text{F}$  as described [198]. Cells were pooled and transferred to petri dishes and kept at 37  $^\circ\text{C}$  in 10 %  $\text{CO}_2$ . One hour after electroporation an equal volume of Dulbecco's modified Eagle's medium pH 7.5, containing 25 mM glucose, 50 UI/ml penicillin, 50  $\mu\text{g}/\text{ml}$  streptomycin, 200 nM phenylisopropyladenosine, 7% (w/v) fatty acid-free bovine serum albumin, and 25 mM HEPES was added. After 18 h of incubation the cells were collected and analyzed.

## Measurement of Elk-1 phosphorylation

The Path-Detect System (Stratagene, CA, USA) was used to assess insulin-stimulated phosphorylation of Elk-1. In this assay, phosphorylation of a transfected GAL4 binding domain/Elk-1 activation domain fusion protein (plasmid: pFA-Elk, 0.5 µg/cuvette) results in activation of a co-transfected GAL4 binding sequence/luciferase reporter plasmid (plasmid: pFR-Luc 1.0 µg/cuvette) resulting in increased luciferase expression. The cells were also transfected with 0.1 µg/cuvette of a plasmid coding for Renilla luciferase; pRluc (BioSignal Packard, CT, USA). Twenty hours after electroporation cells were incubated with 5 nM insulin, for 3 h. The cells were lysed and assayed for firefly and Renilla luciferase using the Dual-Luciferase<sup>®</sup> Reporter Assay Systems, (Promega, WI, USA). Cell lysates were prepared with 200 µl of supplied buffer, by passing through a 25-gauge needle two times. Firefly luciferase assay was initiated by adding 100 µl of Luciferase Assay Reagent II to each 50 µl aliquot of cell lysate. After quantifying the firefly luminescence, the reaction was quenched and the Renilla luciferase reaction was activated by adding 100 µl Stop & Glo<sup>®</sup> Reagent. The firefly and Renilla luciferase activities were measured using a Victor 1420 multilabel counter (Wallac, Turku, Finland). The induced amount of firefly luciferase was normalised according to the constitutively expressed Renilla luciferase, thus correcting for differences in the amount of transfected cells. Different conditions of insulin stimulation were tested, and 5 nM of insulin, given after 20 h (enough time for recombinant production of the Elk-1 fusion protein) was found to increase luciferase production in control cells reproducibly.

## Sample preparations for SDS-PAGE and immunoblotting

For insulin stimulation of ERK1/2 and PKB/Akt phosphorylation, or translocation of HA-tagged GLUT4, cells were incubated with 100 nM insulin, for 10 min at 37 °C. The cells were washed twice in 10 ml of TES buffer (20 mM Tris, 1 mM EDTA, 9% (v/w) sucrose, 0.001% (w/v) fatty acid-free bovine serum albumin) followed by homogenization in 300 µl of 20 mM Tris, 1 mM EDTA, 9% (v/w) sucrose, 8.7 µg/ml PMSF, 0.7 µg/ml pepstatin, 6.5 µg/ml aprotinin, 5 µg/ml leupeptin, 100 nM okadaic acid, 1% (v/v) Triton-X100, and 0.1 % (w/v) SDS, by passing through a 25-gauge needle three times. The lysate was centrifugated at 400 × g for 10 min at 4°C, to pellet cell debris. The protein concentration of the whole-cell lysates was

determined (Protein Assay, Bio-Rad) to allow the same amount of protein to be loaded in each lane during SDS-PAGE.

The purified plasma membrane fraction was obtained from whole-cell lysates by differential and sucrose density gradient centrifugation as described [200, 201].

For immunoprecipitation, the whole-cell lysates were mixed with 3  $\mu\text{g}$  monoclonal antibodies against the HA-tags and the final volume adjusted to 300  $\mu\text{l}$  with TES buffer containing 1 mM  $\text{Na}_3\text{VO}_4$ , 50 mM NaF, 8.7  $\mu\text{g}/\text{ml}$  PMSF, 0.7  $\mu\text{g}/\text{ml}$  pepstatin, 6.5  $\mu\text{g}/\text{ml}$  aprotinin, 5  $\mu\text{g}/\text{ml}$  leupeptin, 100 nM okadaic acid, and 1% (v/v) Triton-X100. The samples were incubated on a rotating wheel at 4  $^\circ\text{C}$ . After 4 h 20  $\mu\text{l}$  of pre-washed protein-G-coupled agarose (Santa Cruz Technology) was added and samples incubated overnight at 4  $^\circ\text{C}$ . After incubation, samples were washed three times with 500  $\mu\text{l}$  of 4  $^\circ\text{C}$  TES buffer containing 1 mM  $\text{Na}_3\text{VO}_4$ , 50 mM NaF, and 1% (v/v) Triton-X100. The whole-cell lysates and immunoprecipitates were boiled with SDS-PAGE sample solution for 5 min, subjected to SDS-PAGE and immunoblotting.

For cells separated according to size, separating cells from medium terminated cell incubations for immunoblotting by centrifugation through dionylphtalate. To minimize post incubation changes in signalling and protein modifications the cells were immediately dissolved in SDS and  $\beta$ -mercaptoethanol with protease and protein phosphatase inhibitors, frozen within 10 s, and thawed in boiling water. Equal amounts of cells as determined by lipocrit, which is total cell volume, was subjected to SDS-PAGE and immunoblotting.

### **SDS-PAGE and immunoblotting**

Equal amount of protein from plasma membrane fractions or whole-cell lysate, or equal amount of cells according to lipocrit from cellsorting, were separated on polyacrylamidegel and electrotranferred onto Immobiline-P (Millipore, Billerica, MA, USA). The membranes were incubated with antibodies as indicated in the text. Bound antibodies were detected with the secondary horseradish peroxidase-conjugated anti-IgG antibody according to

ECL+ protocol (Amersham Biosciences, Amersham, UK), and evaluated by chemiluminescence imaging (Las 1000, Image-Gauge, Fuji, Tokyo, Japan).

### **Fluorescence microscopy**

The transfection efficiency was calculated after electroporation with the plasmid pCIS2 containing cDNA coding for enhanced green fluorescent protein (pCIS2-eGFP) and visualised by fluorescence microscopy (E800 Eclipse microscope, Nikon, Japan). Cells electroporated in PBS buffer without DNA served as negative control (not shown). Representative images were recorded with Image Measurement (Bergstrom Instrument, Solna, Sweden) and the percentage of transfected cells was determined in five viewing fields per sample.

### **Immunofluorescence confocal microscopy of plasma membrane sheets**

Plasma membrane sheets were prepared as described [202] by flushing with ice-cold 150 mM KCl, 1.9 mM Tris/HCl buffer, pH 7.6 and fixed in phosphate-buffer containing 3% paraformaldehyde for 30 min at room temperature. After blocking in bovine serum albumin the membranes were incubated with rabbit anti-IRS1 (20 µg/ml), mouse anti-HA (2 µg/ml) antibodies, or GFP-conjugates as indicated in the text. Primary antibodies were detected with fluorescent secondary antibodies (Highly cross-absorbed Alexa Fluor 488, 594 or 633 diluted 1:500 from Molecular Probes, Carlsbad, CA, USA) by confocal fluorescence microscopy (Nikon Eclipse 800, Nikon, Tokyo, Japan or Leica DMIRE2, Leica, Wetzlar, Germany). Labelling against IRS-1 was measured using the same microscopic and software settings in all experiments allowing for comparison of the amount of IRS-1 between the individual experiments. No labelling was observed in the absence of the primary antibody, nor was any cross-reactivity detected between primary and secondary antibodies. Fluorescent intensity was measured with Scion Image Software (Scion Corporation, MA, USA).

### **Electron microscopy of plasma membrane sheets**

After rinsing adipocytes in ice-cold phosphate buffer (10 mM Na<sub>2</sub>HPO<sub>4</sub>, 1.8 mM KH<sub>2</sub>PO<sub>4</sub>, 137 mM NaCl), the cells attached to gold grids [203]: Poly-L-lysine-formvar-coated grids were rehydrated in ice-cold phosphate buffer

containing the cells. Grids with captured adipocytes were flushed with ice-cold 150 mM KCl, 1.9 mM Tris-HCl buffer, pH 7.4.

Human foreskin fibroblasts were washed as above and then briefly (90 s) treated with hypotonic buffer (50 mM HEPES, pH 7.5) followed by 30 s in poly-L-lysine (1 mg/ml in 150 mM HEPES, pH 7.5), before probe-sonication for 5 s [204].

Plasma membranes remaining on the grids were washed three times in 150 mM HEPES, pH 7.5, and fixed in 0.1 M sodium cacodylate, containing 0.1 M sucrose, 3% paraformaldehyde, and 0.05% glutaraldehyde, for 30 min at room temperature.

Membranes were blocked for 60 min at 37°C with 1% bovine serum albumin (BSA-c, Aurion), 0.1% gelatin, and 1% normal goat serum (Aurion), followed by anti-caveolin antibodies for 2 h at 37°C. Grids were rinsed in phosphate buffer, with 0.15% BSA-c, pH 7.5, before incubation with secondary antibodies. Goat anti-rabbit or anti-mouse IgG, conjugated with 6 or 15 nm colloidal gold, was added to plasma membranes and incubated overnight at 4°C.

After immunolabelling, plasma membranes were rinsed and fixed in 2% glutaraldehyde for 10 min followed by 1% OsO<sub>4</sub> for 30 min in 0.1 M sodium cacodylate, with 0.1 M sucrose, pH 7.5, at room temperature. Grids were rinsed with water, frozen, lyophilized, and coated with 2 nm tungsten by magnetron sputtering directly in the freeze-dryer [205]. Transmission electron microscopy (TEM) was with Jeol EX1200 TEM-SCAN (Tokyo, Japan). Scanning electron microscopy (SEM) was with LEO 1550 Gemini (Zeiss, Oberkochen, Germany).

### **Electron microscopy of intact cells**

Adipocytes were rinsed in ice-cold phosphate buffer and fixed with 2.5% glutaraldehyde and 2% paraformaldehyde in 0.1 M sodium cacodylate for 1 h at room temperature. Cells were attached to grids as above. Cells were then further fixed with 1% OsO<sub>4</sub> in 0.1 M sodium cacodylate, containing 0.1 M sucrose, pH 7.5, for 2 h at room temperature. Grids were rinsed with water, frozen, lyophilized, and coated with 1 nm tungsten by magnetron sputtering

directly in the freeze-dryer [205]. SEM was with LEO 1550 Gemini (Zeiss, Oberkochen, Germany).

### **Immunofluorescence deconvolution microscopy**

Adipocytes were rinsed in phosphate buffer and prefixed in 0.1 M sodium cacodylate containing 3% paraformaldehyde and 0.05% glutaraldehyde for 30 min at room temperature. After treatment with 0.1% NaBH<sub>4</sub> for 15 min unspecific binding was blocked with 1% BSA-c, 0.1% saponin, 0.1% gelatin, 1% normal goat serum (Aurion) for 1 h at 37°C. Cells were then incubated with primary antibodies (rabbit anti-caveolin, 40 µg/ml) in 0.1% saponin for 1.5 h at 37°C. Fluorescent secondary antibody (Alexa fluor 488) was detected by fluorescence microscopy (Axiovert 200M; Zeiss, Göttingen, Germany). Image stacks with number of planes as indicated were collected using Axiovision 3.1 (Zeiss, Göttingen, Germany). Images were deconvoluted using Maximum Likelihood Estimation algorithm by Huygens v2.3.1a-64 software (Scientific Volume Imaging, Hilversrum, The Netherlands). 3D rendering was by Imaris 3.1.3 software (Bitplane AG, Zu-rich, Switzerland). Labelling was not observed in the absence of the primary antibody or in the cross-reactivity between secondary and primary antibodies.

# RESULTS AND DISCUSSION

## Paper I

In this work, we wanted to develop a method for transfection of primary human adipocytes. The technique was based on an existing method for transfection of rat adipocytes by the use of electroporation [198]. The amount of DNA, the carrier plasmid for cDNA, and the strength of the electric pulse were optimized in order to achieve as high transfection efficiency as possible with a relative low cell death. For this, a myc-tagged caveolin construct was used and the recombinant protein expression was analyzed by western blot, using myc-antibodies.

## Results

### Optimization

The cell size is known to be critical for the response to the procedure, and the electric field needed to generate permeabilization of the cell membrane generally increases with decreasing radius of the cell [206]. The large human adipocytes were assumed to require a relative low external field for successful permeabilization. The electric field is adjusted by varying the amplitude (voltage (V)) of the pulse. Too large electric field will cause irreversible damage to the cell membrane leading to cell death. Here, we varied the strength of the pulse between 200-800 V, keeping the number of pulses constant, six, and also the conductance at 25  $\mu$ F, using an exponentially decaying pulse, with 8  $\mu$ g DNA/cuvette. The best expression of myc-tagged caveolin-1 was achieved at 600 V (Figure 5a).

Next the amount of DNA was varied between 0-16  $\mu$ g with the pulses set at 600 V. The highest expression of myc-tagged caveolin-1 was achieved when using 8 and 16  $\mu$ g (Figure 5b). As both 8 and 16  $\mu$ g DNA resulted in high expression, 8  $\mu$ g was chosen to economize the DNA stocks, and therefore used during evaluation of which plasmid carrier to use. Three different plasmids, pCB7, pCIS2 and pCDNA3, all carrying cDNA encoding caveolin-1 were compared and pCIS2 was shown to generate the highest recombinant expression (Figure 5c).

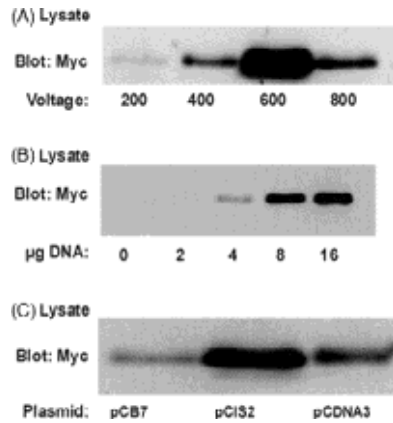


### Figure 5. Optimization

(A) Cells were electroporated with six pulses at 200–800 V at 25  $\mu$ F using 8  $\mu$ g pCIS2-myc-caveolin-1 DNA in each cuvette. (B) The indicated amounts of pCIS2-myc-caveolin-1 cDNA were used for transfection of adipose cells with the voltage set at 600 V. (C) The effect of using different plasmid vectors was tested after subcloning of cDNA for myc-tagged caveolin-1 into pCB7, pCIS2, or pCDNA3. Eight microgram of DNA was added to each cuvette, which was electroporated at 600 V.

The transfection efficiency, ie the number of cells actually expressing recombinant protein was estimated by transfection with enhanced GFP in the pCIS2 vector. Transfected cells that express GFP fluoresce green when exposed to blue light, and were analyzed by fluorescence microscopy. When performing electroporation with the optimized protocol the transfection efficiency was 10-15 % (Figure 6), with a cell viability of approximately 90 %.

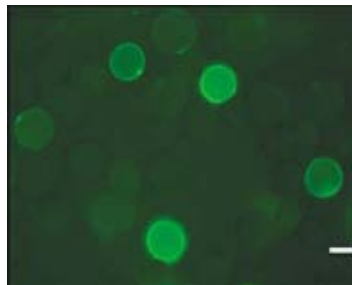


### Figure 6. Transfection efficiency

The transfection efficiency in the human primary adipocytes was determined by transfection of the vector pCIS2 containing cDNA for enhanced green fluorescent protein (eGFP). The mean transfection efficiency was  $15 \pm 5$  % (mean  $\pm$  S.D.). The scale bar corresponds to 50  $\mu$ m.

## Insulin sensitivity

The day after transfection, the insulin-response of the electroporated cells was checked by subjecting whole-cell lysates to SDS-PAGE and transfer to membrane for immunoblotting with phospho-specific antibodies against Akt (metabolic marker) and MAP kinase (mitogenic marker). Insulin stimulation resulted in activation of both Akt and MAP kinase (Figure 7).

The insulin-sensitivity of the transfected cells was checked by expression of HA-tagged Akt and Erk (a MAP kinase). The cells were subjected to immunoprecipitation with HA-antibodies, and the insulin-sensitivity of the recombinant Akt and Erk, was analyzed by SDS-PAGE and immunoblot using phospho-specific antibodies. Also the transfected cells responded to insulin stimulation.

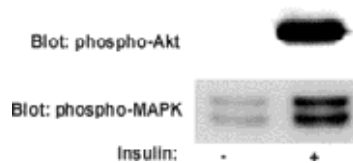


### Figure 7. Insulin sensitivity of electroporated cells

Human adipocytes were electroporated at 600 V and incubated for 20 h. Cells were then stimulated with or without 100 nM of insulin for 10 min and whole-cell lysates were prepared, resolved by SDS-PAGE, and immunoblotted with anti-phospho-PKB/Akt or phospho-MAP-kinase ERK1/2 antibodies as indicated.

## Importance of intact IRS function for insulin-induced signalling

The importance of the IRS for mediating the insulin-induced signalling from the insulin receptor further downstream in primary human adipocytes was demonstrated by the use of the optimized protocol for transfection to express an IRS3 construct. This construct has disrupted binding sites for the regulatory subunit of PI3-kinase (p85) with tyrosine substituted to phenylalanine in four YXXM motifs (IRS3-F4) [175].

The IRS3-F4 mutant was co-transfected with Akt, GLUT4 or Elk-1. Whole-cells lysates from cells co-transfected with IRS3-F4 and Akt were subjected to immunoprecipitation with HA-antibodies, and analyzed by SDS-PAGE and immunoblotting. The expression of HA-tagged Akt was detected with HA-

antibodies. Insulin induced activation of HA-tagged Akt, as detected with phospho-specific antibodies. The insulin-induced activation of Akt was also shown as a shift in the blot detected with HA-antibodies, due to changed mobility during separation in the gel. Co-expression with IRS3-F4 blocked the insulin-induced activation of Akt (Figure 8). Whole-cell lysates were also subjected to SDS-PAGE and immunoblot with Myc-antibodies to ensure expression of the myc-tagged IRS3-F4 (Figure 8).

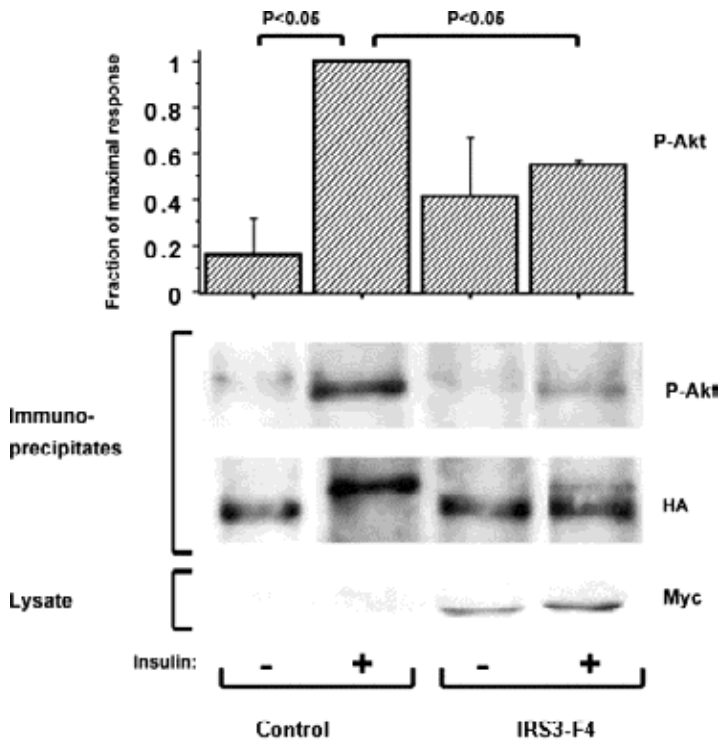


**Figure 8. Effects of expression of IRS3-F4 on insulin activation of PKB/Akt**  
 Empty vector pCIS2 (8  $\mu$ g/cuvette, Control) or IRS3-F4 (8  $\mu$ g/cuvette) were co-transfected with pCIS2-HA-PKB/Akt (0.5  $\mu$ g/cuvette) in human adipocytes and incubated for 20 h. Cells were then stimulated with or without 100 nM insulin for 10 min. Whole-cell lysates were resolved by SDS-PAGE and immunoblotted with anti-myc antibodies. Whole-cell lysates of the transfected adipocytes were also immunoprecipitated with anti-HA antibodies. The immunoprecipitates were subjected to SDS-PAGE and immunoblotted with anti-HA or anti-phospho-PKB/Akt (P-Akt) antibodies, as indicated.

Cells that were transfected with plasmids encoding both IRS3-F4 and HA tagged GLUT4 were subjected to plasma membrane fractionation by sucrose gradient centrifugation to analyze the GLUT4 translocation. The plasma membranes were subjected to SDS-PAGE and immunoblotted with HA-antibodies. Insulin was shown to induce a two-fold increase of GLUT4 at the plasma membrane, while the co-expression of IRS3-F4 inhibited the insulin-induced translocation of HA-GLUT4 (Figure 9).

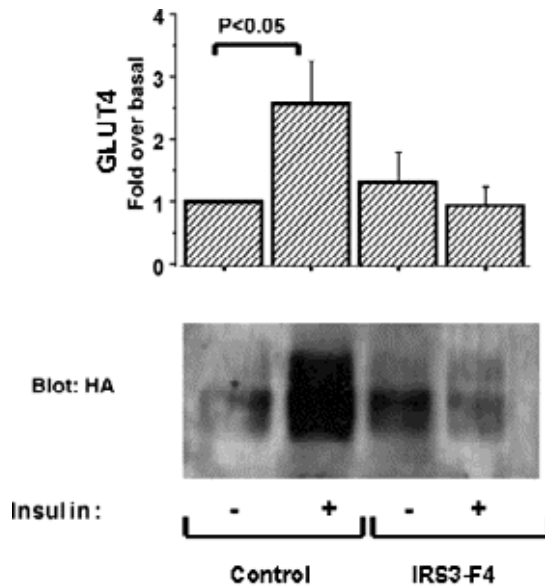


**Figure 9. Effects of expression of IRS3-F4 on insulin stimulated HA-GLUT4 translocation.**

Two micrograms of pCIS2-HA-GLUT4 were co-transfected with 6  $\mu$ g of either empty vector pCIS2 or IRS3-F4. The cells were then stimulated with or without 100 nM of insulin. Plasma membranes were isolated, resolved by SDS-PAGE, and subjected to immunoblotting with anti-HA antibodies.

Elk-1 is a downstream target to the MAP kinase Erk, responsible for regulation of gene transcription control. The insulin-induced activation of Elk-1 was analyzed by a luciferase system, where activation of co-transfected Elk-1 binding domain results in luciferase activity of another co-transfected binding domain/luciferase containing plasmid (see method). Insulin stimulation of Elk-1 in cells co-transfected with IRS3-F4, was totally inhibited.

## Discussion

There are still unanswered questions regarding the mediators and their mechanisms of action in insulin-induced signal transduction, especially in human adipocytes. Techniques to regulate specific proteins at the RNA or protein levels are excellent tools for evaluating the function and importance of molecules in different cellular processes. For studies of insulin signalling at the molecular level, a transfection method for human adipocytes is desirable. Here, we successfully developed a method and optimized a protocol for transfection of primary human adipocytes by electroporation. The 10-15% transfection efficiency of human adipocytes was better than the previously reported 5-10% efficiency of rat adipocytes [198]. The transfected cells remained insulin-sensitive the day after transfection, which makes the method a valuable tool for insulin signal transduction studies. With this technique we demonstrated the importance of properly functional IRS as critical for mediating both metabolic and mitogenic signalling in human adipocytes, with regard to activation of Akt, Elk-1 and translocation of GLUT4. Both the insulin-stimulated metabolic and mitogenic effects were abolished by the interrupted interaction between IRS and PI3-kinase.

It is easy to imagine the difficulty involved in permeabilizing the plasma membrane in primary adipocytes with its extraordinarily thin cytosol, without making irreparable damage to the cell. Fat cells are terminally differentiated cells and do not divide, therefore their chromatin is not as accessible as in dividing cells that in each cells cycle break down the nuclear envelope. This in combination with limited access to fresh human adipocytes probably explains why attempts at transfection of human primary adipocytes have not been reported earlier.

Electroporation is a versatile way for transfection, with the possibility of controlling a number of parameters to suite different circumstances. Actually, electroporation *in vivo* has been described where adipocytes in mice were selectively transfected in situ, making use of the fact that mature adipocyte are much larger than other cells in the adipose tissue [207]. Lately, the equipment for electroporation has been refined with an electric module that truncates the exponential pulse, generating a square wave pulse with a constant voltage [206]. An optimized protocol for transfection of human adipocytes using the square-wave pulse [208] has further simplified the method, while still generating the same transfection efficiency.

## **Paper II**

In this paper, the morphology of intact caveolae structures in primary rat adipocytes was examined with electron microscopic techniques. The localization of the caveolae marker proteins caveolin-1 and -2 within this membrane structure was visualized. The caveolin distribution within the caveolae was confirmed by recombinant expression of myc-tagged caveolin-1 and -2.

### **Results**

#### **Openings of caveolae**

The cell surface from the outside of intact rat adipocytes was examined by scanning electron microscopy (SEM). The surface was shown to be dotted with pores, orifices, with a size of approximate 20 nm. By counting 15 areas of 5 cells, corresponding to 60  $\mu\text{m}^2$  per cell, we calculated that there were about  $6 \times 10^5$  orifices in a cell with the diameter of 100  $\mu\text{m}$ .

#### **Localization of caveolin in caveolae**

The inside of prepared plasma membranes from adipocytes was examined by transmission electron microscopy (TEM) and SEM. The membranes were incubated with caveolin antibodies that were detected with goldconjugated secondary antibodies. Caveolae structures were labelled against caveolin and were shown to protrude from the plasma membrane surface. They varied in size between 25-150 nm in diameter (Figure 10). Close-ups of individual caveolae showed a balloon-like shape connected with the plasma membrane by a narrow neck. By using both mono- and polyclonal antibodies against caveolin, both caveolin-1 and -2 were found to localize to these necks. In the smaller caveolae no necks were detected, but caveolin labelling was restricted to one side of the caveola.

#### **Recombinant expressed caveolin-1 and -2**

To verify our findings, adipocytes were transfected for recombinant expression of myc-tagged caveolin-1 and -2. By detection with myc antibodies, the recombinant myc-tagged caveolin-1 and -2 were also shown to locate in the neck region of caveolae in primary rat adipocytes (Figure 11).

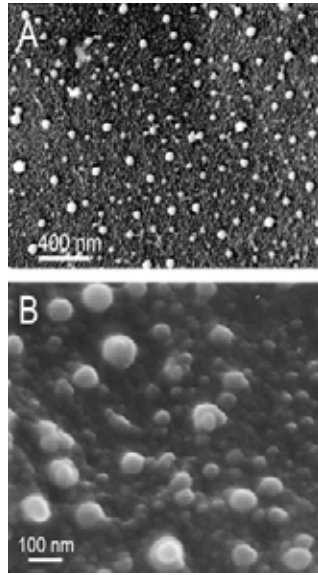


**Figure 10. Electron micrographs of the inside of adipocyte plasma membranes.**

Plasma membrane sheets of freshly isolated adipocytes were prepared attached to grids, cryosputtered and examined by TEM (A) or SEM (B). Images have been contrast inverted.

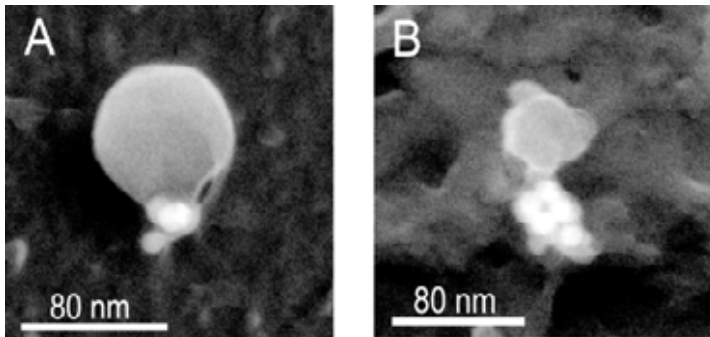


**Figure 11. TEM of caveolae immunogold labelled for myc-tagged caveolin.**

Freshly isolated adipocytes were transfected with C-terminally myc-tagged caveolin-1 (A) or -2 (B). Plasma membrane sheets attached to grids were prepared and immunogold-labelled against the myc-tag, cryosputtered, and examined by TEM. Images have been contrast inverted.

### Caveolin distribution in human fibroblasts

Previous reports of caveolin distribution has described caveolin as forming a striated coat of the caveolar bulb in different cell types, also in human skin fibroblasts [123, 167]. Therefore, we examined the caveolin-1 distribution in human skin fibroblasts in the same way as described for rat adipocytes. We could, however, not find any striated formations. Instead caveolin was found in the membrane proximal region of caveolae. This finding persisted when transfecting the fibroblasts for expression of myc-tagged caveolin-1, which was detected with myc-antibodies (Figure 12).

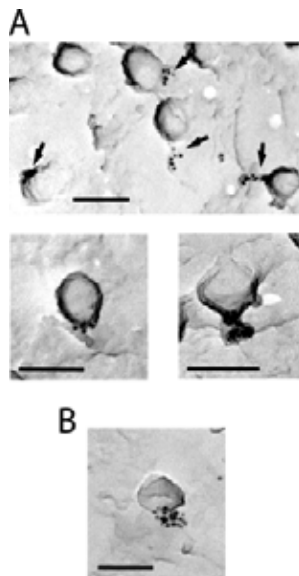


**Figure 12. Caveolae labelled against caveolin in human fibroblasts**

(A) Plasma membrane sheets of the fibroblasts were prepared attached to grids and incubated with antibodies against caveolin for immunogold labelling (6 nm gold). Membranes were then cryosputtered and examined by TEM. (B) Fibroblasts were transfected with carboxy-terminally myc-tagged caveolin-1. Plasma membrane sheets attached to grids were prepared and immunogold-labelled against the myc-tag (6 nm gold), cryosputtered, and examined by TEM. Scale bar, 100 nM.

Previously, cholesterol depletion of the cellular plasma membrane was shown to result in loss of caveolae [135, 140]. Herein, rat adipocytes were  $\beta$ -CD treated to reduce the plasma membrane cholesterol by 50 %. In these cells no caveolae were found at the inner surface. Caveolin were found to be clustered

in the membrane. When examining the outside of the cell surface, the previously identified orifices could not be seen.

## **Discussion**

For the first time small pores, orifices, that constitute caveolae openings on the cell surface, were visualized from the outside of the cell of rat adipocytes. At the inside, caveolae were found of varying sizes. The number of caveolae with cell surface access found at the inner surface corresponded well with the number of orifices found at the cell surface. This demonstrates that most caveolae are connected with the exterior, implying an importance of caveolae for mediating exchange with the extra cellular environment. Caveolin, the marker protein of caveolae, has been described to form a striated coat at the caveolar surface [123, 165]. Later, contradictory results have been published [166], where caveolin was found to locate at distinct regions of the caveolar structure, at the membrane proximal part. In this work, the distribution of caveolin-1 and -2 in freshly isolated rat adipocytes and in human skin fibroblasts, were examined by electron microscopic techniques. Caveolin was shown to be located to the necks of caveolae, rather than the bulbs. This was also found after recombinant expression of both myc-tagged caveolin-1 and caveolin-2, using antibodies against the myc-tag instead of caveolin-1, for detection. For EM studies, we used a cryo-sputter technique where the freeze-drying and magnetron sputtering of the specimen is performed in the same vessel, which benefits the preservation of the structure [205]. The use of different techniques could explain previous reports that have shown caveolin as forming striations at caveolae. The localization of caveolin to the neck supports the idea of caveolin being necessary for stabilization and sequestering the caveolar structure from the rest of the membrane.

## **Paper III**

Previous findings showed IRS1 in human, but not rat, adipocytes to be located at the plasma membrane in non-stimulated cells [93]. In this work we wanted to further investigate the mechanisms behind this species difference. The amount of IRS1 in the plasma membrane from both human and rat adipocytes was analyzed by immunofluorescence microscopy. In response to insulin the IRS1 localization was further examined by cross-transfection and by expressing a chimeric construct.

## **Results**

### **Insulin-regulated IRS1 distribution**

The distribution of IRS1 to the plasma membrane sheets from both human and rat primary adipocytes was detected with IRS1 antibodies using confocal fluorescence microscopy. In absence of insulin, IRS1 was detectable to a large extent in the plasma membrane of human adipocytes, but was barely detected in plasma membranes from rat adipocytes. In human adipocytes, insulin induced a two-fold increase of IRS1 in the plasma membrane. In a corresponding experiment in rat adipocytes, insulin stimulation resulted in a 12-fold increase of IRS1 in the plasma membrane. Interestingly, the amount of IRS in the plasma membranes was similar after insulin stimulation in both human and rat adipocytes (Figure 13).

### **Human IRS1 in rat cells and rat IRS1 in human cells**

We wanted to examine whether the different distribution was due to the IRS1 protein or to the host cell. By electroporation HA-tagged human IRS1 was expressed in rat adipocytes and HA-tagged rat IRS1 was expressed in human adipocytes. HA-antibodies were used for detection of recombinant expressed HA-tagged IRS1 in plasma membranes from transfected, non-stimulated cells. HA-tagged human IRS1 was found at the plasma membrane from rat cells (Figure 14). Endogenous IRS1 in untransfected cells in the same experiment was not labelled with IRS1 antibodies. In contrast, HA-tagged rat IRS1 was not found in plasma membranes from human cells. To identify transfected human cells, rat IRS1 was co-transfected with a plasmid encoding caveolin-1-GFP (Figure 15).

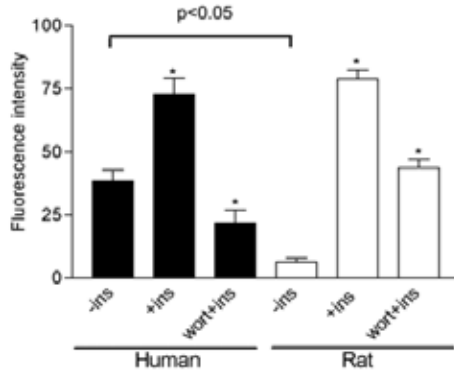


**Figure 13. Effect of insulin and wortmannin on targeting of IRS1 to the plasma membrane of human and rat adipocytes**

Cells were incubated with or without 100 nM insulin for 5 min, in combination with or without pre-treatment with 100 nM of the PI3-kinase inhibitor wortmannin for 30 min prior to insulin-stimulation, as indicated in the figures. Plasma membrane sheets were prepared from human or rat adipocytes for immunofluorescence confocal microscopy. Labelling was performed with primary antibodies against IRS1. The fluorescence intensity was measured and quantified as mean pixel density per area unit in each plasma membrane from three individual experiments (c). \* denotes  $p < 0.05$  compared with basal by Student's t-test, ins denotes insulin, wort denotes wortmannin

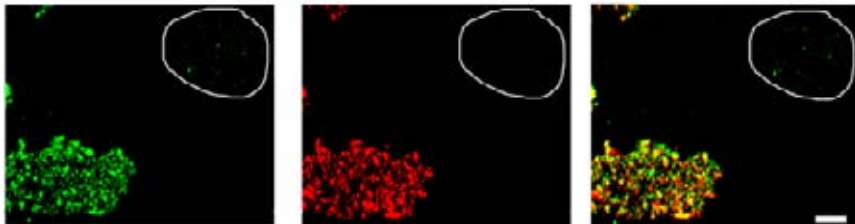


**Figure 14. Recombinant HA-tagged human IRS1 targets the plasma membrane in rat adipocytes.**

Primary epididymal rat adipocytes were transfected with HA-tagged human IRS1 (3  $\mu\text{g}/\text{cuvette}$ ) and plasma membrane sheets were prepared as described in Materials and Methods. The membranes were incubated with antibodies against the HA-tag (shown in green) and IRS1 (shown in red) for immunofluorescence confocal microscopy. The panel shows a transfected cell and the outlined membrane is a non-transfected cell. The scale bar equals 10  $\mu\text{m}$ .

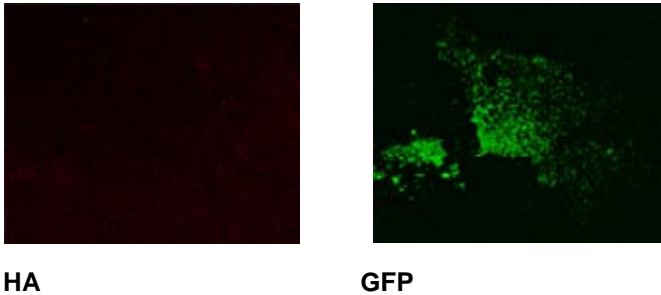


**Figure 15. Localisation of recombinant HA-tagged rat IRS1 expressed in human adipocytes.**

Human adipocytes were transfected with HA-tagged rat IRS1 (3  $\mu\text{g}/\text{cuvette}$ ) and a plasmid encoding a fusion protein of green fluorescent protein (GFP) and caveolin-1 (ccav1-GFP, 2  $\mu\text{g}/\text{cuvette}$ ). Plasma membrane sheets were incubated with antibodies against GFP (shown in green) and the HA-tag (shown in red) for immunofluorescence confocal microscopy.

### **PI3-kinase sensitive translocation**

The importance of PI3-kinase activation and the subsequently produced phosphoinositides for the IRS1 location was examined by treating the cells with wortmannin, a known PI3-kinase inhibitor, prior to insulin-stimulation. By detection with IRS1 antibodies, the inhibition of PI3-kinase was shown to totally block the insulin-induced IRS1 translocation to the plasma membrane in human adipocytes. The amount of IRS1 in the plasma membrane was found to be even lower than in non-insulin-stimulated and non-wortmannin-treated cells. In contrast, inhibition of PI3-kinase in rat adipocytes resulted in an attenuated insulin-induced translocation of IRS1 to the plasma membrane (Figure 13).

### **IRS1 chimer**

A rat IRS1 chimera was created having the last carboxy-terminal 44 amino acids substituted with the corresponding part from human IRS1. The HA-tagged rat IRS1 chimera was co-expressed with caveolin-1-GFP in primary human fat cells, but could not be detected with HA antibodies in the plasma membrane in transfected cells (Figure 16).

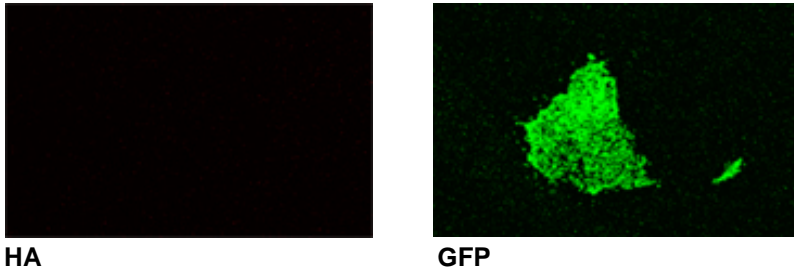


**Figure 16. Localisation of recombinant HA-tagged rat IRS1 with human C-terminus in human adipocytes.**

Human adipocytes were transfected with a HA-tagged rat IRS1 human C-terminus chimera construct (pCIS2-HA-r/h44aa-IRS1, 3  $\mu$ g/cuvette) and a plasmid encoding a fusion protein of green fluorescent protein (GFP) and the membrane targeting protein caveolin-1 (ccav1-GFP, 2  $\mu$ g/cuvette). Plasma membrane sheets were prepared and incubated with antibodies against GFP (shown in green) and HA (shown in red) for confocal immunofluorescence microscopy.

## Discussion

The binding of IRS1 to the plasma membrane has previously been shown to depend on PI3-kinase activation and the subsequently produced phosphoinositides. In the absence of insulin stimulation IRS1 has not been found in the plasma membrane in rat fat cells [94, 96]. However, in human adipocytes we found that IRS1 was located at the plasma membrane in non-stimulated cells and that insulin induced further translocation of IRS1 to the plasma membrane in a PI3-kinase dependent manner. In contrast, IRS1 was in rat adipocytes found at the plasma membrane only after insulin stimulation. The increased translocation of IRS1 to the plasma membrane involved PI3-kinase activity also in the rat cells.

It is interesting that IRS1 is translocated to the plasma membrane to the same maximal level in both human and rat adipocytes, although this involved only a doubling of plasma membrane localized IRS1 in the human cells. The difference between IRS1 in human and rat cells indicates that the subcellular localization of rat IRS1 differs from the human IRS1 regarding its membrane binding properties. The variable response to wortmannin could be due to different binding affinity towards PI3-kinase produced lipid products. By

expression of human IRS1 in rat fat cells and vice versa, we showed that the binding of human IRS1 to the plasma membrane is a property of the human IRS1 protein.

The PH and PTB domains of the human and rat IRS1 are identical. Therefore other parts of the sequence or perhaps specific residues outside these domains could be critical for membrane targeting [87]. Taylor et al [92] showed that a full-length IRS1 fused with GFP was translocated to the plasma membrane in response to insulin. However, the amino-terminal part fused with GFP was located to the plasma membrane in non-stimulated cells, which suggests the carboxy-terminal part of IRS1 to inhibit the targeting of IRS1 to the plasma membrane in the absence of insulin [92]. The c-terminal part of IRS1 contains a proline-rich sequence, which in the human IRS1 constitutes a PI3-kinase binding site (PxxP) not present in the rat IRS1, which could contribute to the different subcellular localization in some way. We examined the role of the c-terminus of IRS1 by substituting the last 44 carboxy-terminal amino acids in the rat IRS1 with the corresponding sequence of human IRS1. As this did not affect binding of the rat IRS1 to the plasma membrane this sequence alone does apparently not confer plasma membrane binding. It is obviously of importance to further examine the scattered differences in the rat and human sequences of IRS1 for their impact on IRS1 targeting. It should be borne in mind, though, that a specific amino acid sequence not only can confer binding of the human protein, but may also block the rat protein from interaction with the plasma membrane. Our findings stress the importance of performing studies in human cells in order to understand insulin signalling in human beings.

The role of the cytoskeleton for the subcellular localization of IRS1 was recently investigated by Thomas et al 2006 [209]. The cytoskeleton network has previously been shown to be necessary for the insulin-induced glucose uptake in terms of GLUT4 translocation to the plasma membrane [210-212]. One could expect the cytoskeleton to be involved in the regulation of the IRS proteins. Interestingly, Thomas et al presented data that indicated the subcellular localization and function of IRS1 actually did not depend on cytoskeleton integrity.



## **Paper IV**

Obesity is closely linked to insulin resistance and type II diabetes, and large fat cells are proposed to be less responsive to insulin than small [48, 51, 52]. To examine the importance of the size of fat cells for their insulin sensitivity, we compared the insulin responsiveness of large and small cells obtained from the same individual.

### **Results**

#### **Method for separation**

Previous methods for separation of adipocytes from the same individual were based on varying buoyancy depending on cell size. The method presented by Björntorp et al [58] was relatively complicated. A recent report of separation has combined the flotation and filtering techniques [59], where a cell suspension was kept in a tube, and cells that had reached the surface after 30 s were collected. After repeated flotation both the fraction of cells collected at the surface and the remaining cells in the tube, were filtered through nylon mesh to attain two fractions. However, this method requires very large amounts of fat tissue [59]. Here, we developed a technique to separate the cells by filtration, rendering two fractions of fat cells; small and large adipocytes (see method).

#### **Insulin sensitivity in small and large cells**

Plasma membrane sheets from the adipocytes were analyzed by immunofluorescence confocal microscopy with GLUT4 antibodies, and the amount of GLUT4 quantified as a measurement of insulin sensitivity. Interestingly, insulin induced the amount of GLUT4 at the plasma membrane to increase 2 fold in the small cells, compared with the large cells, where insulin actually did not affect the amount of GLUT4 translocated to the plasma membrane (Figure 17). Notably, the insulin-induced increase of GLUT4 at the plasma membrane in small cells accorded well with previous reports with unsorted adipocytes [139, 199].

#### **Amount of insulin receptor, IRS1 and caveolin-1**

The amounts of insulin receptor and IRS1 in whole-cell lysates were analyzed by SDS-PAGE and immunoblotting with antibodies against insulin receptor and IRS1. The amount of insulin receptor and IRS1 were similar in the two cell fractions. Plasma membranes were analyzed with confocal microscopy

using antibodies against caveolin. Caveolin levels increases as fat cells differentiate from preadipocytes and increase in size. However, quantification of caveolin in the plasma membrane using immunofluorescence microscopy revealed that both cell size populations had similar amounts of caveolin per surface area.

### Insulin-induced activation of Akt

The insulin-induced activation of Akt was analyzed by SDS-PAGE and immunoblotting with phospho-specific antibodies. Insulin resulted in a 2-fold activation of Akt in both small and large cells.

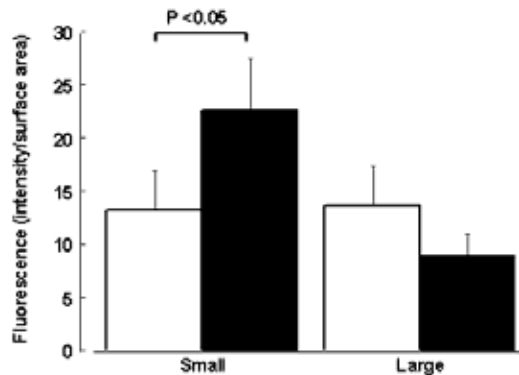


**Figure 17. Translocation of GLUT4 to the plasma membrane in small and large cells in response to insulin**

Human cells were sorted in two populations, small and large. The cells were treated with or without 10 nM insulin for 30 min and plasma membrane sheets prepared for immunolabelling with anti GLUT4 antibodies for immunofluorescence microscopy. The fluorescence intensity was measured and quantified as mean pixel density per area unit.

## Discussion

In this work, we developed a method for separating small and large cells from the same subject, by filtration. The two cell fractions, small and large cells, were analyzed for their insulin sensitivity by assessing GLUT4 translocation. The increased translocation of GLUT4 at the plasma membrane in response to insulin in small fat cells, which was not found in the large cells, supports the notion that small cells are more sensitive to the effects of insulin to promote glucose uptake than large cells and indeed suggests that the glucose uptake

mainly takes place in the smaller fat cells. This finding is in line with anti-diabetic drugs based on activation of PPAR- $\gamma$ , which improves the insulin sensitivity by enhancing glucose uptake and lipid accumulation while increasing the number of small adipocytes [213], probably due to loss of large cells by apoptosis and differentiation of new small adipocytes from adipocyte precursors.

Large fat cells necessarily have to have an impaired ability to increase the storage of fat but are also resistant to the anti-lipolytic effect of insulin, resulting in an increased fatty acids release [5]. This leads to elevated levels of circulating fatty acids affecting the liver, muscle and  $\beta$ -cells, thus aggravating the insulin resistance [5]. The anti-lipolytic effect of insulin is proposed to be mediated by the activation of Akt, which in turn activates phosphodiesterase 3B and thereby reduces cAMP levels and inhibits the hormone-sensitive lipase. However, we found no difference between the phosphorylation of Akt in small and large cells, which may be due to the relatively high concentration of insulin used.

A population of very small fat cells (VSFC) has been reported to be lost during the digestion with collagenase [214]. After cell size fractionation we did not see many VSFC ( $< 25 \mu\text{m}$  in diameter), maybe because they are lost during the digestion. However, our method for filtration of cells produces a significant separation of large and small cells, but the VSFC could represent yet another group of fat cells that is of importance for the insulin-sensitivity in vivo.

## CONCLUSIONS

A protocol for transfection of primary human adipocytes by electroporation was developed and optimized. With a transfection efficiency of 10-15 %, the cells remained insulin-sensitive for further analysis the day after transfection. The usefulness of the protocol was demonstrated in several molecular biological applications.

Functional IRS was crucial for mediation of both metabolic and mitogenic signalling in human adipocytes. Human IRS1 was demonstrated to be located at the plasma membrane in human adipocytes under basal non-stimulated conditions as a result of the properties of the human protein, rather than any special condition in the human cells.

Caveolae in rat adipocytes were found to be connected to the exterior by a narrow neck, appearing as orifices at the cell surface. Caveolin-1 and -2, as well as tagged recombinant expressed caveolin-1 and -2, were located to the necks of caveolae, and did not cover the surface of the caveolar bulb.

We developed a method to sort small and large primary human adipocytes from the same individual. Large cells were found to be insulin resistant with regard to GLUT4 translocation in response to insulin.

## ACKNOWLEDGEMENTS

I would like to thank all of you who have, in some way or the other, contributed to my work with this thesis.

Especially I would like to thank:

My supervisor **Fredrik Nyström** and co-supervisor **Peter Strålfors**. Your scientific knowledge and never ending enthusiasm has inspired me during this time! Thank you for everything!

**Gunilla Westermark**, for believing in me!

**Hans Thorn**, who taught me the microscope techniques. It was pleasant having you around! Thanks a lot!

**Unn Örtegren**, my former room and Qi-gong mate (and free-diver instructor, I still try to practice some “tömma-masken-under vattnet”, without success). Thank you for your friendship!

**Veronika Patcha Brodin** for your friendship and hospitality during those years. I guess you are the only one who supports my interest in horses... Keep up the spirit!

**Nabila Aboulaich**, former room mate who will succeed over there (also). You are such a nice person!

**Johan Paulsson** who has brought a lot of joy to floor 12. It's never boring around you!

**Sofia Nyström**, for your sensibility. Your appearance has a soothing effect, needed between the ups and downs in the lab!

**Elisabeth Hallin**, for all help! You are superb!

**Anita Öst**, for being nice to me! And smart! I'm sorry we didn't have the time to run a project together.

**Niclas Franck**, for being a nice co-worker, good luck with your thesis.

**Lilian Sauma**, for being sweet and helpful! You will find your ways.

**Anna Danielsson**, for being a nice person, good luck with your work!

**Jesper Svartz**, you made a persistent performance at Hans Thorns party. If you get tired of teaching, why don't consider Dramaten? You are something extraordinary!

**Johanna Gustavsson**, for your scientific discussions and for your support in life.

**Mats Söderström**, for always taking your time to answer my questions, I appreciated that.

**Santiago Parpal**, for being a nice co-worker and friend!

**Margareta Karlsson**, who taught me a lot about cellbiology in “the beginning”. Keep on singing!

**Kristina Loinder**, for sharing your base group experiences and for taking care of Elvis.

**Eva Särndahl, Pia Druid**, thank you!

**Jana, Tobias, Siri, Sebastian**, I'm sorry I didn't have the chance to get to know you better but I wish you all good luck!

**Per Bengtsson**, who never hesitated to start a party!

All present and former students and co-workers at floor 12 at, or somewhere close to, Cellbiologen.

**All people at KFC, Örebro**, my second lab family! Thank you for making it possible for me to complete my work “at your place”. And thanks for all support and encouragement!

**Helle and Marie** (or should I write Jock and Miss Ellie?) It’s strange how you two end up together in everything! Thank you for adding a non-scientific dimension, I guess it’s time for me to finish my other thesis now...?

To all of you in “**föräldragänget**”, I promise to be more involved in the future planning of children’s birthday parties, dinners and so on! Thank you for not getting tired of my absence.

All relatives and friends, eventually it’s done!

My parents, **Staffan** and **Gunilla**, sister **Anna** and brother **Johan**, for endless support.

**Hanna** and **Oscar**, who remind me of what’s valuable in life.

**Johan!** Who manage to live with me and to deal with all my ideas about everything! You are marvellous!

We thank doctors P. Kjolhede, K. Crafoord, P. Sandström, B. Lönnberg, S. Halili and G. Andreescu for supplying fat tissue during surgery. Financial support was from Lions Foundation, Gamla Tjänarinnor, Östergötland County Council, Swedish Medical Society, University Hospital of Linköping Research Funds, Lars Hierta, Diabetes Research Centre, Swedish Diabetes Association, Swedish Foundation for Strategic Research (National Network for Cardiovascular Research), Swedish Research Council, and the Swedish National Board for Laboratory Animals.

## REFERENCES

1. Zimmet, P., K.G. Alberti, and J. Shaw, *Global and societal implications of the diabetes epidemic*. Nature, 2001. **414**(6865): p. 782-7.
2. *Report of the Expert Committee on the Diagnosis and Classification of Diabetes Mellitus*. Diabetes Care, 1997. **20**(7): p. 1183-97.
3. Kahn, S.E., *The relative contributions of insulin resistance and beta-cell dysfunction to the pathophysiology of Type 2 diabetes*. Diabetologia, 2003. **46**(1): p. 3-19.
4. Schinner, S., et al., *Molecular mechanisms of insulin resistance*. Diabet Med, 2005. **22**(6): p. 674-82.
5. DeFronzo, R.A., *Dysfunctional fat cells, lipotoxicity and type 2 diabetes*. Int J Clin Pract Suppl, 2004(143): p. 9-21.
6. DeFronzo, R.A., *Pathogenesis of type 2 diabetes mellitus*. Med Clin North Am, 2004. **88**(4): p. 787-835, ix.
7. Romsos, D.R. and G.A. Leveille, *Effect of diet on activity of enzymes involved in fatty acid and cholesterol synthesis*. Adv Lipid Res, 1974. **12**(0): p. 97-146.
8. Diraison, F., et al., *Differences in the regulation of adipose tissue and liver lipogenesis by carbohydrates in humans*. J Lipid Res, 2003. **44**(4): p. 846-53.
9. Anthonsen, M.W., et al., *Identification of novel phosphorylation sites in hormone-sensitive lipase that are phosphorylated in response to isoproterenol and govern activation properties in vitro*. J Biol Chem, 1998. **273**(1): p. 215-21.
10. Belfrage, P., et al., *Regulation of adipose-tissue lipolysis by phosphorylation of hormone-sensitive lipase*. Int J Obes, 1981. **5**(6): p. 635-41.
11. Stralfors, P. and R.C. Honnor, *Insulin-induced dephosphorylation of hormone-sensitive lipase. Correlation with lipolysis and cAMP-dependent protein kinase activity*. Eur J Biochem, 1989. **182**(2): p. 379-85.
12. Stralfors, P., P. Bjorgell, and P. Belfrage, *Hormonal regulation of hormone-sensitive lipase in intact adipocytes: identification of phosphorylated sites and effects on the phosphorylation by lipolytic hormones and insulin*. Proc Natl Acad Sci U S A, 1984. **81**(11): p. 3317-21.
13. Carey, V.J., et al., *Body fat distribution and risk of non-insulin-dependent diabetes mellitus in women. The Nurses' Health Study*. Am J Epidemiol, 1997. **145**(7): p. 614-9.
14. Pi-Sunyer, F.X., *Weight and non-insulin-dependent diabetes mellitus*. Am J Clin Nutr, 1996. **63**(3 Suppl): p. 426S-429S.
15. Harris, M.I., et al., *Prevalence of diabetes, impaired fasting glucose, and impaired glucose tolerance in U.S. adults. The Third National Health and Nutrition Examination Survey, 1988-1994*. Diabetes Care, 1998. **21**(4): p. 518-24.
16. DeFronzo, R.A., *Lilly lecture 1987. The triumvirate: beta-cell, muscle, liver. A collusion responsible for NIDDM*. Diabetes, 1988. **37**(6): p. 667-87.
17. Bjorntorp, P., *Metabolic implications of body fat distribution*. Diabetes Care, 1991. **14**(12): p. 1132-43.
18. Chan, J.M., et al., *Obesity, fat distribution, and weight gain as risk factors for clinical diabetes in men*. Diabetes Care, 1994. **17**(9): p. 961-9.

19. Kissebah, A.H. and A.N. Peiris, *Biology of regional body fat distribution: relationship to non-insulin-dependent diabetes mellitus*. *Diabetes Metab Rev*, 1989. **5**(2): p. 83-109.
20. Albu, J.B., A.J. Kovera, and J.A. Johnson, *Fat distribution and health in obesity*. *Ann N Y Acad Sci*, 2000. **904**: p. 491-501.
21. Arner, P., et al., *Beta-adrenoceptor expression in human fat cells from different regions*. *J Clin Invest*, 1990. **86**(5): p. 1595-600.
22. Arner, P., *Regional adiposity in man*. *J Endocrinol*, 1997. **155**(2): p. 191-2.
23. Lafontan, M. and M. Berlan, *Do regional differences in adipocyte biology provide new pathophysiological insights?* *Trends Pharmacol Sci*, 2003. **24**(6): p. 276-83.
24. Bolinder, J., et al., *Differences at the receptor and postreceptor levels between human omental and subcutaneous adipose tissue in the action of insulin on lipolysis*. *Diabetes*, 1983. **32**(2): p. 117-23.
25. Boden, G. and G.I. Shulman, *Free fatty acids in obesity and type 2 diabetes: defining their role in the development of insulin resistance and beta-cell dysfunction*. *Eur J Clin Invest*, 2002. **32 Suppl 3**: p. 14-23.
26. Boden, G., *Role of fatty acids in the pathogenesis of insulin resistance and NIDDM*. *Diabetes*, 1997. **46**(1): p. 3-10.
27. Golay, A., et al., *Metabolic basis of obesity and noninsulin-dependent diabetes mellitus*. *Diabetes Metab Rev*, 1988. **4**(8): p. 727-47.
28. McGarry, J.D., *Banting lecture 2001: dysregulation of fatty acid metabolism in the etiology of type 2 diabetes*. *Diabetes*, 2002. **51**(1): p. 7-18.
29. Thorne, A., et al., *A pilot study of long-term effects of a novel obesity treatment: omentectomy in connection with adjustable gastric banding*. *Int J Obes Relat Metab Disord*, 2002. **26**(2): p. 193-9.
30. Klein, S., et al., *Absence of an effect of liposuction on insulin action and risk factors for coronary heart disease*. *N Engl J Med*, 2004. **350**(25): p. 2549-57.
31. Rosen, E.D., et al., *PPAR gamma is required for the differentiation of adipose tissue in vivo and in vitro*. *Mol Cell*, 1999. **4**(4): p. 611-7.
32. Miyazaki, Y., et al., *Effect of rosiglitazone on glucose and non-esterified fatty acid metabolism in Type II diabetic patients*. *Diabetologia*, 2001. **44**(12): p. 2210-9.
33. Olefsky, J.M., *Treatment of insulin resistance with peroxisome proliferator-activated receptor gamma agonists*. *J Clin Invest*, 2000. **106**(4): p. 467-72.
34. Kelly, I.E., et al., *Effects of a thiazolidinedione compound on body fat and fat distribution of patients with type 2 diabetes*. *Diabetes Care*, 1999. **22**(2): p. 288-93.
35. Miyazaki, Y., et al., *Effect of pioglitazone on abdominal fat distribution and insulin sensitivity in type 2 diabetic patients*. *J Clin Endocrinol Metab*, 2002. **87**(6): p. 2784-91.
36. Mori, Y., et al., *Effect of troglitazone on body fat distribution in type 2 diabetic patients*. *Diabetes Care*, 1999. **22**(6): p. 908-12.
37. Maggs, D.G., et al., *Metabolic effects of troglitazone monotherapy in type 2 diabetes mellitus. A randomized, double-blind, placebo-controlled trial*. *Ann Intern Med*, 1998. **128**(3): p. 176-85.
38. Sauma, L., et al., *Peroxisome proliferator activated receptor gamma activity is low in mature primary human visceral adipocytes*. *Diabetologia*, 2006.

39. Alessi, M.C., et al., *Production of plasminogen activator inhibitor 1 by human adipose tissue: possible link between visceral fat accumulation and vascular disease*. *Diabetes*, 1997. **46**(5): p. 860-7.
40. Hotamisligil, G.S., N.S. Shargill, and B.M. Spiegelman, *Adipose expression of tumor necrosis factor- $\alpha$ : direct role in obesity-linked insulin resistance*. *Science*, 1993. **259**(5091): p. 87-91.
41. Bajaj, M., et al., *Plasma resistin concentration, hepatic fat content, and hepatic and peripheral insulin resistance in pioglitazone-treated type II diabetic patients*. *Int J Obes Relat Metab Disord*, 2004. **28**(6): p. 783-9.
42. Yamauchi, T., et al., *The fat-derived hormone adiponectin reverses insulin resistance associated with both lipodystrophy and obesity*. *Nat Med*, 2001. **7**(8): p. 941-6.
43. Pradhan, A.D., et al., *C-reactive protein, interleukin 6, and risk of developing type 2 diabetes mellitus*. *Jama*, 2001. **286**(3): p. 327-34.
44. Rondinone, C.M., *Adipocyte-derived hormones, cytokines, and mediators*. *Endocrine*, 2006. **29**(1): p. 81-90.
45. Mora, S. and J.E. Pessin, *An adipocentric view of signaling and intracellular trafficking*. *Diabetes Metab Res Rev*, 2002. **18**(5): p. 345-56.
46. Abel, E.D., et al., *Adipose-selective targeting of the GLUT4 gene impairs insulin action in muscle and liver*. *Nature*, 2001. **409**(6821): p. 729-33.
47. Dietze, D., et al., *Impairment of insulin signaling in human skeletal muscle cells by co-culture with human adipocytes*. *Diabetes*, 2002. **51**(8): p. 2369-76.
48. Salans, L.B., J.L. Knittle, and J. Hirsch, *The role of adipose cell size and adipose tissue insulin sensitivity in the carbohydrate intolerance of human obesity*. *J Clin Invest*, 1968. **47**(1): p. 153-165.
49. Bjorntorp, P., A. Jonsson, and P. Berchtold, *Adipose tissue cellularity in maturity onset diabetes mellitus*. *Acta Med Scand*, 1972. **191**(1-2): p. 129-32.
50. Avram, M.M., A.S. Avram, and W.D. James, *Subcutaneous fat in normal and diseased states: 1. Introduction*. *J Am Acad Dermatol*, 2005. **53**(4): p. 663-70.
51. Weyer, C., et al., *Enlarged subcutaneous abdominal adipocyte size, but not obesity itself, predicts type II diabetes independent of insulin resistance*. *Diabetologia*, 2000. **43**(12): p. 1498-506.
52. Smith, U., *Studies of human adipose tissue in culture. I. Incorporation of glucose and release of glycerol*. *Anat Rec*, 1972. **172**(4): p. 597-602.
53. Salans, L.B. and J.W. Dougherty, *The effect of insulin upon glucose metabolism by adipose cells of different size. Influence of cell lipid and protein content, age, and nutritional state*. *J Clin Invest*, 1971. **50**(7): p. 1399-410.
54. Buren, J., et al., *In vitro reversal of hyperglycemia normalizes insulin action in fat cells from type 2 diabetes patients: is cellular insulin resistance caused by glucotoxicity in vivo?* *Metabolism*, 2003. **52**(2): p. 239-45.
55. Fried, S.K., D.A. Bunkin, and A.S. Greenberg, *Omental and subcutaneous adipose tissues of obese subjects release interleukin-6: depot difference and regulation by glucocorticoid*. *J Clin Endocrinol Metab*, 1998. **83**(3): p. 847-50.
56. Sopasakis, V.R., et al., *High local concentrations and effects on differentiation implicate interleukin-6 as a paracrine regulator*. *Obes Res*, 2004. **12**(3): p. 454-60.
57. Giorgino, F., L. Laviola, and J.W. Eriksson, *Regional differences of insulin action in adipose tissue: insights from in vivo and in vitro studies*. *Acta Physiol Scand*, 2005. **183**(1): p. 13-30.

58. Bjorntorp, P. and L. Sjostrom, *Fat cell size and number in adipose tissue in relation to metabolism*. *Isr J Med Sci*, 1972. **8**(3): p. 320-4.
59. Jernas, M., et al., *Separation of human adipocytes by size: hypertrophic fat cells display distinct gene expression*. *Faseb J*, 2006. **20**(9): p. 1540-2.
60. Czech, M.P., *The nature and regulation of the insulin receptor: structure and function*. *Annu Rev Physiol*, 1985. **47**: p. 357-81.
61. Bevan, P., *Insulin signalling*. *J Cell Sci*, 2001. **114**(Pt 8): p. 1429-30.
62. White, M.F., *The insulin signalling system and the IRS proteins*. *Diabetologia*, 1997. **40 Suppl 2**: p. S2-17.
63. Smith, U., *Impaired ('diabetic') insulin signaling and action occur in fat cells long before glucose intolerance--is insulin resistance initiated in the adipose tissue?* *Int J Obes Relat Metab Disord*, 2002. **26**(7): p. 897-904.
64. Danielsson, A., et al., *Insulin resistance in human adipocytes occurs downstream of IRS1 after surgical cell isolation but at the level of phosphorylation of IRS1 in type 2 diabetes*. *Febs J*, 2005. **272**(1): p. 141-51.
65. Rondinone, C.M., et al., *Insulin receptor substrate (IRS) 1 is reduced and IRS-2 is the main docking protein for phosphatidylinositol 3-kinase in adipocytes from subjects with non-insulin-dependent diabetes mellitus*. *Proc Natl Acad Sci U S A*, 1997. **94**(8): p. 4171-5.
66. Danielsson, A., et al., *Attenuation of insulin-stimulated insulin receptor substrate-1 serine 307 phosphorylation in insulin resistance of type 2 diabetes*. *J Biol Chem*, 2005. **280**(41): p. 34389-92.
67. White, M.F., *IRS proteins and the common path to diabetes*. *Am J Physiol Endocrinol Metab*, 2002. **283**(3): p. E413-22.
68. Tamemoto, H., et al., *Insulin resistance and growth retardation in mice lacking insulin receptor substrate-1*. *Nature*, 1994. **372**(6502): p. 182-6.
69. Araki, E., et al., *Alternative pathway of insulin signalling in mice with targeted disruption of the IRS-1 gene*. *Nature*, 1994. **372**(6502): p. 186-90.
70. Withers, D.J., et al., *Disruption of IRS-2 causes type 2 diabetes in mice*. *Nature*, 1998. **391**(6670): p. 900-4.
71. Kubota, N., et al., *Disruption of insulin receptor substrate 2 causes type 2 diabetes because of liver insulin resistance and lack of compensatory beta-cell hyperplasia*. *Diabetes*, 2000. **49**(11): p. 1880-9.
72. Liu, S.C., et al., *Insulin receptor substrate 3 is not essential for growth or glucose homeostasis*. *J Biol Chem*, 1999. **274**(25): p. 18093-9.
73. Fantin, V.R., et al., *Mice lacking insulin receptor substrate 4 exhibit mild defects in growth, reproduction, and glucose homeostasis*. *Am J Physiol Endocrinol Metab*, 2000. **278**(1): p. E127-33.
74. Kido, Y., et al., *Tissue-specific insulin resistance in mice with mutations in the insulin receptor, IRS-1, and IRS-2*. *J Clin Invest*, 2000. **105**(2): p. 199-205.
75. Kadowaki, T., et al., *Insulin resistance and growth retardation in mice lacking insulin receptor substrate-1 and identification of insulin receptor substrate-2*. *Diabet Med*, 1996. **13**(9 Suppl 6): p. S103-8.
76. Sesti, G., et al., *Defects of the insulin receptor substrate (IRS) system in human metabolic disorders*. *Faseb J*, 2001. **15**(12): p. 2099-111.
77. Giovannone, B., et al., *Insulin receptor substrate (IRS) transduction system: distinct and overlapping signaling potential*. *Diabetes Metab Res Rev*, 2000. **16**(6): p. 434-41.
78. Kerouz, N.J., et al., *Differential regulation of insulin receptor substrates-1 and -2 (IRS-1 and IRS-2) and phosphatidylinositol 3-kinase isoforms in liver and*

- muscle of the obese diabetic (ob/ob) mouse.* J Clin Invest, 1997. **100**(12): p. 3164-72.
79. Lavan, B.E. and G.E. Lienhard, *The insulin-elicited 60-kDa phosphotyrosine protein in rat adipocytes is associated with phosphatidylinositol 3-kinase.* J Biol Chem, 1993. **268**(8): p. 5921-8.
  80. Lavan, B.E., W.S. Lane, and G.E. Lienhard, *The 60-kDa phosphotyrosine protein in insulin-treated adipocytes is a new member of the insulin receptor substrate family.* J Biol Chem, 1997. **272**(17): p. 11439-43.
  81. Kaburagi, Y., et al., *Role of insulin receptor substrate-1 and pp60 in the regulation of insulin-induced glucose transport and GLUT4 translocation in primary adipocytes.* J Biol Chem, 1997. **272**(41): p. 25839-44.
  82. Bjornholm, M., et al., *Absence of functional insulin receptor substrate-3 (IRS-3) gene in humans.* Diabetologia, 2002. **45**(12): p. 1697-702.
  83. Yenush, L., et al., *The pleckstrin homology domain is the principal link between the insulin receptor and IRS-1.* J Biol Chem, 1996. **271**(39): p. 24300-6.
  84. Eck, M.J., et al., *Structure of the IRS-1 PTB domain bound to the juxtamembrane region of the insulin receptor.* Cell, 1996. **85**(5): p. 695-705.
  85. Wolf, G., et al., *PTB domains of IRS-1 and Shc have distinct but overlapping binding specificities.* J Biol Chem, 1995. **270**(46): p. 27407-10.
  86. Kaburagi, Y., et al., *Insulin-independent and wortmannin-resistant targeting of IRS-3 to the plasma membrane via its pleckstrin homology domain mediates a different interaction with the insulin receptor from that of IRS-1.* Diabetologia, 2001. **44**(8): p. 992-1004.
  87. Virkamaki, A., K. Ueki, and C.R. Kahn, *Protein-protein interaction in insulin signaling and the molecular mechanisms of insulin resistance.* J Clin Invest, 1999. **103**(7): p. 931-43.
  88. Dhe-Paganon, S., et al., *Crystal structure of the pleckstrin homology-phosphotyrosine binding (PH-PTB) targeting region of insulin receptor substrate 1.* Proc Natl Acad Sci U S A, 1999. **96**(15): p. 8378-83.
  89. White, M.F., *The IRS-signalling system: a network of docking proteins that mediate insulin action.* Mol Cell Biochem, 1998. **182**(1-2): p. 3-11.
  90. Razzini, G., et al., *Different subcellular localization and phosphoinositides binding of insulin receptor substrate protein pleckstrin homology domains.* Mol Endocrinol, 2000. **14**(6): p. 823-36.
  91. Maffucci, T., et al., *Role of pleckstrin homology domain in regulating membrane targeting and metabolic function of insulin receptor substrate 3.* Mol Endocrinol, 2003. **17**(8): p. 1568-79.
  92. Jacobs, A.R., D. LeRoith, and S.I. Taylor, *Insulin receptor substrate-1 pleckstrin homology and phosphotyrosine-binding domains are both involved in plasma membrane targeting.* J Biol Chem, 2001. **276**(44): p. 40795-802.
  93. Karlsson, M., et al., *Colocalization of insulin receptor and insulin receptor substrate-1 to caveolae in primary human adipocytes. Cholesterol depletion blocks insulin signalling for metabolic and mitogenic control.* Eur J Biochem, 2004. **271**(12): p. 2471-9.
  94. Inoue, G., et al., *Dynamics of insulin signaling in 3T3-L1 adipocytes. Differential compartmentalization and trafficking of insulin receptor substrate (IRS)-1 and IRS-2.* J Biol Chem, 1998. **273**(19): p. 11548-55.

95. Kriauciunas, K.M., M.G. Myers, Jr., and C.R. Kahn, *Cellular compartmentalization in insulin action: altered signaling by a lipid-modified IRS-1*. *Mol Cell Biol*, 2000. **20**(18): p. 6849-59.
96. Clark, S.F., et al., *Intracellular localization of phosphatidylinositide 3-kinase and insulin receptor substrate-1 in adipocytes: potential involvement of a membrane skeleton*. *J Cell Biol*, 1998. **140**(5): p. 1211-25.
97. Zick, Y., *Uncoupling insulin signalling by serine/threonine phosphorylation: a molecular basis for insulin resistance*. *Biochem Soc Trans*, 2004. **32**(Pt 5): p. 812-6.
98. Tanti, J.F., et al., *Alteration in insulin action: role of IRS-1 serine phosphorylation in the retroregulation of insulin signalling*. *Ann Endocrinol (Paris)*, 2004. **65**(1): p. 43-8.
99. Pirola, L., A.M. Johnston, and E. Van Obberghen, *Modulation of insulin action*. *Diabetologia*, 2004. **47**(2): p. 170-84.
100. Danielsson, A., F.H. Nystrom, and P. Stralfors, *Phosphorylation of IRS1 at serine 307 and serine 312 in response to insulin in human adipocytes*. *Biochem Biophys Res Commun*, 2006. **342**(4): p. 1183-7.
101. Alessi, D.R. and P. Cohen, *Mechanism of activation and function of protein kinase B*. *Curr Opin Genet Dev*, 1998. **8**(1): p. 55-62.
102. Andjelkovic, M., et al., *Role of translocation in the activation and function of protein kinase B*. *J Biol Chem*, 1997. **272**(50): p. 31515-24.
103. Khan, A.H. and J.E. Pessin, *Insulin regulation of glucose uptake: a complex interplay of intracellular signalling pathways*. *Diabetologia*, 2002. **45**(11): p. 1475-83.
104. Saltiel, A.R. and J.E. Pessin, *Insulin signaling in microdomains of the plasma membrane*. *Traffic*, 2003. **4**(11): p. 711-6.
105. Saltiel, A.R. and J.E. Pessin, *Insulin signaling pathways in time and space*. *Trends Cell Biol*, 2002. **12**(2): p. 65-71.
106. Chiang, S.H., et al., *Insulin-stimulated GLUT4 translocation requires the CAP-dependent activation of TC10*. *Nature*, 2001. **410**(6831): p. 944-8.
107. Roberts, T.M., *Cell biology. A signal chain of events*. *Nature*, 1992. **360**(6404): p. 534-5.
108. Ogawa, W., T. Matozaki, and M. Kasuga, *Role of binding proteins to IRS-1 in insulin signalling*. *Mol Cell Biochem*, 1998. **182**(1-2): p. 13-22.
109. Joost, H.G. and B. Thorens, *The extended GLUT-family of sugar/polyol transport facilitators: nomenclature, sequence characteristics, and potential function of its novel members (review)*. *Mol Membr Biol*, 2001. **18**(4): p. 247-56.
110. Watson, R.T. and J.E. Pessin, *Subcellular compartmentalization and trafficking of the insulin-responsive glucose transporter, GLUT4*. *Exp Cell Res*, 2001. **271**(1): p. 75-83.
111. Karnieli, E., et al., *Insulin-stimulated translocation of glucose transport systems in the isolated rat adipose cell. Time course, reversal, insulin concentration dependency, and relationship to glucose transport activity*. *J Biol Chem*, 1981. **256**(10): p. 4772-7.
112. James, D.E., R.C. Piper, and J.W. Slot, *Targeting of mammalian glucose transporters*. *J Cell Sci*, 1993. **104** ( Pt 3): p. 607-12.
113. Pessin, J.E., et al., *Molecular basis of insulin-stimulated GLUT4 vesicle trafficking. Location! Location! Location!* *J Biol Chem*, 1999. **274**(5): p. 2593-6.

114. Simpson, F., J.P. Whitehead, and D.E. James, *GLUT4--at the cross roads between membrane trafficking and signal transduction*. Traffic, 2001. **2**(1): p. 2-11.
115. Palade, G.E., *Fine structure of blood capillaries*. J Appl Physics, 1953. **24**: p. 1424.
116. Yamada, E., *The fine structure of the gall bladder epithelium of the mouse*. J Biophys Biochem Cytol, 1955. **1**(5): p. 445-58.
117. Bruns, R.R. and G.E. Palade, *Studies on blood capillaries. I. General organization of blood capillaries in muscle*. J Cell Biol, 1968. **37**(2): p. 244-76.
118. Forbes, M.S., M.L. Rennels, and E. Nelson, *Caveolar systems and sarcoplasmic reticulum in coronary smooth muscle cells of the mouse*. J Ultrastruct Res, 1979. **67**(3): p. 325-39.
119. Bretscher, M.S. and S. Whytock, *Membrane-associated vesicles in fibroblasts*. J Ultrastruct Res, 1977. **61**(2): p. 215-7.
120. Cushman, S.W., *Structure-function relationships in the adipose cell. I. Ultrastructure of the isolated adipose cell*. J Cell Biol, 1970. **46**(2): p. 326-41.
121. Cushman, S.W., *Structure-function relationships in the adipose cell. II. Pinocytosis and factors influencing its activity in the isolated adipose cell*. J Cell Biol, 1970. **46**(2): p. 342-53.
122. Thorn, H., et al., *Cell surface orifices of caveolae and localization of caveolin to the necks of caveolae in adipocytes*. Mol Biol Cell, 2003. **14**(10): p. 3967-76.
123. Rothberg, K.G., et al., *Caveolin, a protein component of caveolae membrane coats*. Cell, 1992. **68**(4): p. 673-82.
124. Iwabuchi, K., K. Handa, and S. Hakomori, *Separation of glycosphingolipid-enriched microdomains from caveolar membrane characterized by presence of caveolin*. Methods Enzymol, 2000. **312**: p. 488-94.
125. Smart, E.J., et al., *A detergent-free method for purifying caveolae membrane from tissue culture cells*. Proc Natl Acad Sci U S A, 1995. **92**(22): p. 10104-8.
126. Shu, L., et al., *Caveolar structure and protein sorting are maintained in NIH 3T3 cells independent of glycosphingolipid depletion*. Arch Biochem Biophys, 2000. **373**(1): p. 83-90.
127. Ortegren, U., et al., *Lipids and glycosphingolipids in caveolae and surrounding plasma membrane of primary rat adipocytes*. Eur J Biochem, 2004. **271**(10): p. 2028-36.
128. Fujimoto, T., et al., *Caveolae: from a morphological point of view*. J Electron Microsc (Tokyo), 1998. **47**(5): p. 451-60.
129. Simons, K. and E. Ikonen, *Functional rafts in cell membranes*. Nature, 1997. **387**(6633): p. 569-72.
130. Simionescu, N., M. Simionescu, and G.E. Palade, *Permeability of muscle capillaries to small heme-peptides. Evidence for the existence of patent transendothelial channels*. J Cell Biol, 1975. **64**(3): p. 586-607.
131. Stang, E., J. Kartenbeck, and R.G. Parton, *Major histocompatibility complex class I molecules mediate association of SV40 with caveolae*. Mol Biol Cell, 1997. **8**(1): p. 47-57.
132. Fielding, C.J. and P.E. Fielding, *Caveolae and intracellular trafficking of cholesterol*. Adv Drug Deliv Rev, 2001. **49**(3): p. 251-64.
133. Ost, A., et al., *Triacylglycerol is synthesized in a specific subclass of caveolae in primary adipocytes*. J Biol Chem, 2005. **280**(1): p. 5-8.

134. Goldberg, R.I., R.M. Smith, and L. Jarett, *Insulin and alpha 2-macroglobulin-methylamine undergo endocytosis by different mechanisms in rat adipocytes: I. Comparison of cell surface events.* J Cell Physiol, 1987. **133**(2): p. 203-12.
135. Gustavsson, J., et al., *Localization of the insulin receptor in caveolae of adipocyte plasma membrane.* Faseb J, 1999. **13**(14): p. 1961-71.
136. Feng, Y., et al., *VEGF-induced permeability increase is mediated by caveolae.* Invest Ophthalmol Vis Sci, 1999. **40**(1): p. 157-67.
137. Liu, P., et al., *Localization of platelet-derived growth factor-stimulated phosphorylation cascade to caveolae.* J Biol Chem, 1996. **271**(17): p. 10299-303.
138. Mineo, C., et al., *Localization of epidermal growth factor-stimulated Ras/Raf-1 interaction to caveolae membrane.* J Biol Chem, 1996. **271**(20): p. 11930-5.
139. Gustavsson, J., S. Parpal, and P. Stralfors, *Insulin-stimulated glucose uptake involves the transition of glucose transporters to a caveolae-rich fraction within the plasma membrane: implications for type II diabetes.* Mol Med, 1996. **2**(3): p. 367-72.
140. Parpal, S., et al., *Cholesterol depletion disrupts caveolae and insulin receptor signaling for metabolic control via insulin receptor substrate-1, but not for mitogen-activated protein kinase control.* J Biol Chem, 2001. **276**(13): p. 9670-8.
141. Glenney, J.R., Jr., *Tyrosine phosphorylation of a 22-kDa protein is correlated with transformation by Rous sarcoma virus.* J Biol Chem, 1989. **264**(34): p. 20163-6.
142. Kurzchalia, T.V., et al., *VIP21, a 21-kD membrane protein is an integral component of trans-Golgi-network-derived transport vesicles.* J Cell Biol, 1992. **118**(5): p. 1003-14.
143. Scherer, P.E., et al., *Caveolin isoforms differ in their N-terminal protein sequence and subcellular distribution. Identification and epitope mapping of an isoform-specific monoclonal antibody probe.* J Biol Chem, 1995. **270**(27): p. 16395-401.
144. Kogo, H. and T. Fujimoto, *Caveolin-1 isoforms are encoded by distinct mRNAs. Identification Of mouse caveolin-1 mRNA variants caused by alternative transcription initiation and splicing.* FEBS Lett, 2000. **465**(2-3): p. 119-23.
145. Scherer, P.E., et al., *Identification, sequence, and expression of caveolin-2 defines a caveolin gene family.* Proc Natl Acad Sci U S A, 1996. **93**(1): p. 131-5.
146. Scherer, P.E., et al., *Cell-type and tissue-specific expression of caveolin-2. Caveolins 1 and 2 co-localize and form a stable hetero-oligomeric complex in vivo.* J Biol Chem, 1997. **272**(46): p. 29337-46.
147. Tang, Z., et al., *Molecular cloning of caveolin-3, a novel member of the caveolin gene family expressed predominantly in muscle.* J Biol Chem, 1996. **271**(4): p. 2255-61.
148. Okamoto, T., et al., *Caveolins, a family of scaffolding proteins for organizing "preassembled signaling complexes" at the plasma membrane.* J Biol Chem, 1998. **273**(10): p. 5419-22.
149. Sargiacomo, M., et al., *Oligomeric structure of caveolin: implications for caveolae membrane organization.* Proc Natl Acad Sci U S A, 1995. **92**(20): p. 9407-11.

150. Das, K., et al., *The membrane-spanning domains of caveolins-1 and -2 mediate the formation of caveolin hetero-oligomers. Implications for the assembly of caveolae membranes in vivo.* J Biol Chem, 1999. **274**(26): p. 18721-8.
151. Mora, R., et al., *Caveolin-2 localizes to the golgi complex but redistributes to plasma membrane, caveolae, and rafts when co-expressed with caveolin-1.* J Biol Chem, 1999. **274**(36): p. 25708-17.
152. Couet, J., et al., *Identification of peptide and protein ligands for the caveolin-scaffolding domain. Implications for the interaction of caveolin with caveolae-associated proteins.* J Biol Chem, 1997. **272**(10): p. 6525-33.
153. Couet, J., M. Sargiacomo, and M.P. Lisanti, *Interaction of a receptor tyrosine kinase, EGF-R, with caveolins. Caveolin binding negatively regulates tyrosine and serine/threonine kinase activities.* J Biol Chem, 1997. **272**(48): p. 30429-38.
154. Schlegel, A. and M.P. Lisanti, *A molecular dissection of caveolin-1 membrane attachment and oligomerization. Two separate regions of the caveolin-1 C-terminal domain mediate membrane binding and oligomer/oligomer interactions in vivo.* J Biol Chem, 2000. **275**(28): p. 21605-17.
155. Schlegel, A., et al., *A role for the caveolin scaffolding domain in mediating the membrane attachment of caveolin-1. The caveolin scaffolding domain is both necessary and sufficient for membrane binding in vitro.* J Biol Chem, 1999. **274**(32): p. 22660-7.
156. Yamamoto, M., et al., *Caveolin is an activator of insulin receptor signaling.* J Biol Chem, 1998. **273**(41): p. 26962-8.
157. Nystrom, F.H., et al., *Caveolin-1 interacts with the insulin receptor and can differentially modulate insulin signaling in transfected Cos-7 cells and rat adipose cells.* Mol Endocrinol, 1999. **13**(12): p. 2013-24.
158. Drab, M., et al., *Loss of caveolae, vascular dysfunction, and pulmonary defects in caveolin-1 gene-disrupted mice.* Science, 2001. **293**(5539): p. 2449-52.
159. Razani, B. and M.P. Lisanti, *Caveolin-deficient mice: insights into caveolar function human disease.* J Clin Invest, 2001. **108**(11): p. 1553-61.
160. Cohen, A.W., et al., *Caveolin-1-deficient mice show insulin resistance and defective insulin receptor protein expression in adipose tissue.* Am J Physiol Cell Physiol, 2003. **285**(1): p. C222-35.
161. Murata, M., et al., *VIP21/caveolin is a cholesterol-binding protein.* Proc Natl Acad Sci U S A, 1995. **92**(22): p. 10339-43.
162. Dietzen, D.J., W.R. Hastings, and D.M. Lublin, *Caveolin is palmitoylated on multiple cysteine residues. Palmitoylation is not necessary for localization of caveolin to caveolae.* J Biol Chem, 1995. **270**(12): p. 6838-42.
163. Uittenbogaard, A. and E.J. Smart, *Palmitoylation of caveolin-1 is required for cholesterol binding, chaperone complex formation, and rapid transport of cholesterol to caveolae.* J Biol Chem, 2000. **275**(33): p. 25595-9.
164. Machleidt, T., et al., *Multiple domains in caveolin-1 control its intracellular traffic.* J Cell Biol, 2000. **148**(1): p. 17-28.
165. Peters, K.R., W.W. Carley, and G.E. Palade, *Endothelial plasmalemmal vesicles have a characteristic striped bipolar surface structure.* J Cell Biol, 1985. **101**(6): p. 2233-8.
166. Westermann, M., H. Leutbecher, and H.W. Meyer, *Membrane structure of caveolae and isolated caveolin-rich vesicles.* Histochem Cell Biol, 1999. **111**(1): p. 71-81.

167. Anderson, R.G., *Caveolae: where incoming and outgoing messengers meet*. Proc Natl Acad Sci U S A, 1993. **90**(23): p. 10909-13.
168. Bell, P.B., Jr., M. Lindroth, and B.A. Fredriksson, *Use of sputter coating to prepare whole mounts of cytoskeletons for transmission and high-resolution scanning and scanning transmission electron microscopy*. J Electron Microscop Tech, 1987. **7**(3): p. 149-59.
169. Nabi, I.R. and P.U. Le, *Caveolae/raft-dependent endocytosis*. J Cell Biol, 2003. **161**(4): p. 673-7.
170. Fra, A.M., et al., *De novo formation of caveolae in lymphocytes by expression of VIP21-caveolin*. Proc Natl Acad Sci U S A, 1995. **92**(19): p. 8655-9.
171. Li, S., et al., *Baculovirus-based expression of mammalian caveolin in Sf21 insect cells. A model system for the biochemical and morphological study of caveolae biogenesis*. J Biol Chem, 1996. **271**(45): p. 28647-54.
172. Razani, B., et al., *Caveolin-2-deficient mice show evidence of severe pulmonary dysfunction without disruption of caveolae*. Mol Cell Biol, 2002. **22**(7): p. 2329-44.
173. Tagawa, A., et al., *Assembly and trafficking of caveolar domains in the cell: caveolae as stable, cargo-triggered, vesicular transporters*. J Cell Biol, 2005. **170**(5): p. 769-79.
174. Kurreck, J., *Antisense technologies. Improvement through novel chemical modifications*. Eur J Biochem, 2003. **270**(8): p. 1628-44.
175. Zhou, L., et al., *Action of insulin receptor substrate-3 (IRS-3) and IRS-4 to stimulate translocation of GLUT4 in rat adipose cells*. Mol Endocrinol, 1999. **13**(3): p. 505-14.
176. Quon, M.J., et al., *Insulin receptor substrate 1 mediates the stimulatory effect of insulin on GLUT4 translocation in transfected rat adipose cells*. J Biol Chem, 1994. **269**(45): p. 27920-4.
177. Zhou, L., et al., *Insulin receptor substrate-2 (IRS-2) can mediate the action of insulin to stimulate translocation of GLUT4 to the cell surface in rat adipose cells*. J Biol Chem, 1997. **272**(47): p. 29829-33.
178. Shigematsu, S., et al., *The adipocyte plasma membrane caveolin functional/structural organization is necessary for the efficient endocytosis of GLUT4*. J Biol Chem, 2003. **278**(12): p. 10683-90.
179. Sasaki, K., M. Sato, and Y. Umezawa, *Fluorescent indicators for Akt/protein kinase B and dynamics of Akt activity visualized in living cells*. J Biol Chem, 2003. **278**(33): p. 30945-51.
180. Sato, M., et al., *Fluorescent indicators for imaging protein phosphorylation in single living cells*. Nat Biotechnol, 2002. **20**(3): p. 287-94.
181. Pelkmans, L., J. Kartenbeck, and A. Helenius, *Caveolar endocytosis of simian virus 40 reveals a new two-step vesicular-transport pathway to the ER*. Nat Cell Biol, 2001. **3**(5): p. 473-83.
182. Song, L., et al., *Electric field-induced molecular vibration for noninvasive, high-efficiency DNA transfection*. Mol Ther, 2004. **9**(4): p. 607-16.
183. Chen, C. and H. Okayama, *High-efficiency transformation of mammalian cells by plasmid DNA*. Mol Cell Biol, 1987. **7**(8): p. 2745-52.
184. Diacumakos, E.G., *Methods for micromanipulation of human somatic cells in culture*. Methods Cell Biol, 1973. **7**: p. 287-311.
185. Felgner, P.L., et al., *Lipofection: a highly efficient, lipid-mediated DNA-transfection procedure*. Proc Natl Acad Sci U S A, 1987. **84**(21): p. 7413-7.

186. Neumann, E., et al., *Gene transfer into mouse lyoma cells by electroporation in high electric fields*. *Embo J*, 1982. **1**(7): p. 841-5.
187. Okino, M. and H. Mohri, *Effects of a high-voltage electrical impulse and an anticancer drug on in vivo growing tumors*. *Jpn J Cancer Res*, 1987. **78**(12): p. 1319-21.
188. Heller, R., et al., *In vivo gene electroinjection and expression in rat liver*. *FEBS Lett*, 1996. **389**(3): p. 225-8.
189. Melvik, J.E., et al., *Increase in cis-dichlorodiammineplatinum (II) cytotoxicity upon reversible electroporabilization of the plasma membrane in cultured human NHIK 3025 cells*. *Eur J Cancer Clin Oncol*, 1986. **22**(12): p. 1523-30.
190. Neumann, E., S. Kakorin, and K. Toensing, *Fundamentals of electroporative delivery of drugs and genes*. *Bioelectrochem Bioenerg*, 1999. **48**(1): p. 3-16.
191. Weaver, J.C., *Molecular basis for cell membrane electroporation*. *Ann N Y Acad Sci*, 1994. **720**: p. 141-52.
192. Sukharev, S.I., et al., *Electroporation and electrophoretic DNA transfer into cells. The effect of DNA interaction with electropores*. *Biophys J*, 1992. **63**(5): p. 1320-7.
193. Rols, M.P., et al., *Control by ATP and ADP of voltage-induced mammalian-cell-membrane permeabilization, gene transfer and resulting expression*. *Eur J Biochem*, 1998. **254**(2): p. 382-8.
194. Hebert, E., *Improvement of exogenous DNA nuclear importation by nuclear localization signal-bearing vectors: a promising way for non-viral gene therapy?* *Biol Cell*, 2003. **95**(2): p. 59-68.
195. Mora, S., et al., *NCS-1 inhibits insulin-stimulated GLUT4 translocation in 3T3L1 adipocytes through a phosphatidylinositol 4-kinase-dependent pathway*. *J Biol Chem*, 2002. **277**(30): p. 27494-500.
196. van Dam, E.M., R. Govers, and D.E. James, *Akt activation is required at a late stage of insulin-induced GLUT4 translocation to the plasma membrane*. *Mol Endocrinol*, 2005. **19**(4): p. 1067-77.
197. Shigematsu, S., S.L. Miller, and J.E. Pessin, *Differentiated 3T3L1 adipocytes are composed of heterogenous cell populations with distinct receptor tyrosine kinase signaling properties*. *J Biol Chem*, 2001. **276**(18): p. 15292-7.
198. Quon, M.J., et al., *Transfection of DNA into isolated rat adipose cells by electroporation: evaluation of promoter activity in transfected adipose cells which are highly responsive to insulin after one day in culture*. *Biochem Biophys Res Commun*, 1993. **194**(1): p. 338-46.
199. Stenkula, K.G., et al., *Expression of a mutant IRS inhibits metabolic and mitogenic signalling of insulin in human adipocytes*. *Mol Cell Endocrinol*, 2004. **221**(1-2): p. 1-8.
200. McKeel, D.W. and L. Jarett, *Preparation and characterization of a plasma membrane fraction from isolated fat cells*. *J Cell Biol*, 1970. **44**(2): p. 417-32.
201. Oka, Y. and M.P. Czech, *Photoaffinity labeling of insulin-sensitive hexose transporters in intact rat adipocytes. Direct evidence that latent transporters become exposed to the extracellular space in response to insulin*. *J Biol Chem*, 1984. **259**(13): p. 8125-33.
202. Thorn, H., et al., *Cell surface orifices of caveolae and localization of caveolin to the necks of caveolae in adipocytes*, in *Mol Biol Cell*. 2003. p. 3967-76.
203. Voldstedlund, M., J. Tranum-Jensen, and J. Vinten, *Quantitation of Na<sup>+</sup>/K<sup>+</sup>-ATPase and glucose transporter isoforms in rat adipocyte plasma membrane by immunogold labeling*. *J Membr Biol*, 1993. **136**(1): p. 63-73.

204. Robinson, L.J., et al., *Translocation of the glucose transporter (GLUT4) to the cell surface in permeabilized 3T3-L1 adipocytes: effects of ATP insulin, and GTP gamma S and localization of GLUT4 to clathrin lattices.* J Cell Biol, 1992. **117**(6): p. 1181-96.
205. Lindroth, M., B.A. Fredriksson, and P.B. Bell, *Cryosputtering--a combined freeze-drying and sputtering method for high-resolution electron microscopy.* J Microsc, 1991. **161**(Pt 2): p. 229-39.
206. Gehl, J., *Electroporation: theory and methods, perspectives for drug delivery, gene therapy and research.* Acta Physiol Scand, 2003. **177**(4): p. 437-47.
207. Granneman, J.G., et al., *Seeing the trees in the forest: selective electroporation of adipocytes within adipose tissue.* Am J Physiol Endocrinol Metab, 2004. **287**(3): p. E574-82.
208. Sauma, L., et al., *PPAR-gamma response element activity in intact primary human adipocytes: effects of fatty acids.* Nutrition, 2006. **22**(1): p. 60-8.
209. Thomas, E.C., et al., *The subcellular fractionation properties and function of insulin receptor substrate-1 (IRS-1) are independent of cytoskeletal integrity.* Int J Biochem Cell Biol, 2006. **38**(10): p. 1686-99.
210. Kanzaki, M. and J.E. Pessin, *Insulin-stimulated GLUT4 translocation in adipocytes is dependent upon cortical actin remodeling.* J Biol Chem, 2001. **276**(45): p. 42436-44.
211. Wang, Q., et al., *Protein kinase B/Akt participates in GLUT4 translocation by insulin in L6 myoblasts.* Mol Cell Biol, 1999. **19**(6): p. 4008-18.
212. Omata, W., et al., *Actin filaments play a critical role in insulin-induced exocytotic recruitment but not in endocytosis of GLUT4 in isolated rat adipocytes.* Biochem J, 2000. **346 Pt 2**: p. 321-8.
213. Boden, G. and M. Zhang, *Recent findings concerning thiazolidinediones in the treatment of diabetes.* Expert Opin Investig Drugs, 2006. **15**(3): p. 243-50.
214. Julien, P., J.P. Despres, and A. Angel, *Scanning electron microscopy of very small fat cells and mature fat cells in human obesity.* J Lipid Res, 1989. **30**(2): p. 293-9.